

**ENERGY DISCHARGE CAPABILITY OF SURGE
ARRESTER FOR 132 KV DOUBLE CIRCUIT
TRANSMISSION LINE IN MALAYSIA**

NOR HIDAYAH BINTI HAJI NOR HASSAN

**DISSERTATION SUBMITTED IN FULFILMENT
OF THE REQUIREMENTS FOR THE DEGREE OF
MASTER OF ENGINEERING SCIENCE**

**FACULTY OF ENGINEERING
UNIVERSITY OF MALAYA
KUALA LUMPUR**

2018

UNIVERSITY MALAYA

ORIGINAL LITERARY WORK DECLARATION

Name of Candidate: **Nor Hidayah binti Haji Nor Hassan**

Registration/Matric No: **KGA110025**

Name of Degree: Master of Engineering Science

Title of Project Paper/Research Report/Dissertation/Thesis (“this Work”):

Energy Discharge Capability of Surge Arrester for 132 kV Double Circuit Transmission Line in Malaysia

Field of Study: **Power System**

I do solemnly and sincerely declare that:

- (1) I am the sole author/writer of this Work;
- (2) This Work is original;
- (3) Any use of any work in which copyright exists was done by way of fair dealing and for permitted purposes and any excerpt or extract from, or reference to or reproduction of any copyright work has been disclosed expressly and sufficiently and the title of the work and its authorship have been acknowledged in this work;
- (4) I hereby assign all and every rights in the copyright to this work to the University of Malaya (“UM”), who henceforth shall be owner of the copyright in this work and that any reproduction or use in any form or by any means whatsoever is prohibited without the written consent of UM having been first had and obtained;
- (5) I am fully aware that if in the course of making this Work I have infringed any copyright whether intentionally or otherwise, i may be subject to legal action or any other action as may be determined by UM

Candidate’s Signature:

Date:

Subscribed and solemnly declared before,

Witness’s Signature:

Date:

Name:

Designation:

ENERGY DISCHARGE CAPABILITY OF SURGE ARRESTER FOR 132 KV DOUBLE CIRCUIT TRANSMISSION LINE IN MALAYSIA

ABSTRACT

Lightning overvoltage has been identified as the major problem of overhead transmission lines tripping in Malaysia due to high incidence of keraunic activities. Improving lightning performance of the lines is crucial to avoid physical damage to the system equipment, which may result in service interruptions to the electricity consumers. Based on the studies conducted by the national utility company, application of surge arresters has been proven to be the most effective way in providing optimum lightning protection of a transmission line. Thus, in this work, the capability of surge arresters installed on a 132 kV double circuit transmission line in withstanding current and energy discharged by lightning strikes during back flashover phenomena is studied. Several surge arrester configurations and placement were simulated using Electromagnetic Transient Program (EMTP-RV) to determine the most effective protection design based on the actual tripping pattern recorded by Lightning Detection System (LDS) in Malaysia. Installing surge arresters at each phase conductor has been found to completely eliminate double circuit transmission line tripping due to back flashover. Some design parameters such as tower footing resistance, span length and phase conductor angle were varied to analyse their significance on the surge arrester discharged energy. The results indicate that increasing tower footing resistance, current magnitude and number of towers result in the surge arresters to discharge higher energy. It can be deduced that the designed surge arresters comply with the energy capability requirement of 5.1 kJ/kV as specified by the national utility company and are able to provide sufficient lightning protection on transmission lines.

ABSTRAK

Kilat voltan lampau dikenalpasti sebagai punca utama kepada masalah gangguan bekalan talian penghantaran di Malaysia disebabkan oleh kadar aktiviti 'isokeraunic' yang tinggi. Memperbaiki prestasi kilat pada talian adalah penting bagi mengelakkan kerosakan fizikal kepada peralatan dalam sistem, yang boleh mengakibatkan gangguan bekalan kepada pengguna-pengguna elektrik. Berdasarkan kajian yang dijalankan oleh syarikat utiliti kebangsaan, aplikasi penangkap kilat merupakan cara terbaik dalam memberikan perlindungan yang optimum kepada talian penghantaran. Oleh itu, kajian ini bertujuan untuk menyiasat keupayaan penangkap kilat yang dipasang pada litar berkembar dua talian penghantaran 132 kV, dalam menahan arus dan tenaga yang dinyahcas oleh kilat ketika terjadinya fenomena 'back flashover'. Beberapa konfigurasi dan penempatan penangkap kilat disimulasi menggunakan perisian Electromagnetic Transient Program (EMTP-RV) bagi menentukan reka bentuk perlindungan yang paling berkesan berdasarkan pola kegagalan yang direkodkan oleh Sistem Pengesanan Kilat (LDS) di Malaysia. Pemasangan penangkap kilat pada setiap pengalir fasa didapati dapat menghapuskan sepenuhnya kegagalan litar berkembar dua talian penghantaran yang diakibatkan oleh 'back flashover'. Beberapa parameter seperti rintangan kaki menara, panjang rentang talian dan sudut fasa konduktor di ubah untuk menganalisa kesannya pada tenaga dinyahcas oleh penangkap kilat. Keputusan menunjukkan bahawa peningkatan rintangan kaki menara, magnitud kilat dan bilangan menara menyebabkan tenaga dinyahcas oleh penangkap kilat lebih tinggi. Ia boleh disimpulkan bahawa penangkap kilat yang direka mematuhi keperluan keupayaan tenaga 5.1 kJ/kV sebagaimana yang dinyatakan oleh syarikat utiliti nasional dan dapat menyediakan perlindungan kilat yang mencukupi untuk talian penghantaran

ACKNOWLEDGEMENT

First and foremost, I am expressing my appreciation and praise to God for His Guidance and blessings throughout my entire studies in University of Malaya. I like to sincerely thank Prof. Dr. Ab. Halim bin Abu Bakar and Dr. Hazlee Azil bin Illias, my supervisors, who contributed a lot towards the accomplishment of my research and work for guiding, monitoring and teaching me throughout the whole duration of the research.

I also would like to express my sincere gratitude towards Syahirah, Alyaa, Aisyah, Hazwani and my lab members for their constant source of help in terms of sharing technical information and opinion whenever I need for advice. Without their help it would be difficult for me to accomplish the dissertation.

I wish to thank Prof. Dr Hazlie bin Mokhlis of the UM Power System Research Group, who has been very supportive of me throughout my study.

My appreciation is extended to my family and friends who provided a great assistance in terms of materials, effort and ideas, directly or indirectly, blessings and encouragement. To my parents, thank you for having faith in me that I will be able to make it. Thank you for your affectionate love and support. Lastly, may all of efforts will be blessed with great rewards from the Almighty Allah.

TABLE OF CONTENTS

Title	Page
Declaration	ii
Abstract	iii
Abstrak	iv
Acknowledgements	v
Table of contents	vi
List of tables	x
List of figures	xi
List of abbreviations	xiii
CHAPTER 1: INTRODUCTION	1
1.1 Introduction	1
1.2 Problem Statement	3
1.3 Thesis Objectives	4
1.4 Contribution of the Thesis	4
1.5 Organization of the Thesis	5
CHAPTER 2: LITERATURE REVIEW	7
2.1 Transmission Line	7
2.2 Lightning Phenomena at Transmission Line	9
2.2.1 Back Flashover Event	9
2.2.2 Shielding Failure Flashover Event	11

2.3	Lightning Surge Analysis Methods on Transmission Lines	12
2.3.1	Field Data	12
2.3.2	Back Flashover Rate	13
2.3.3	Simulation Methods	13
2.4	Factors Affecting Flashover Patterns	14
2.4.1	Line Parameters	15
2.4.2	Lightning Current Parameters	15
2.4.3	Transmission Tower Parameters	21
2.4.4	Tower Footing Resistance	24
2.4.5	Insulator String	24
2.5	Protection of Transmission Lines	25
2.5.1	Surge Arrester	25
2.5.2	Arrester Discharge Energy	26
CHAPTER 3: RESEARCH METHODOLOGY		28
3.1	Introduction	28
3.1.1	Introduction of EMTP Simulation Software	28
3.1.2	Test System	29
3.2	Modeling of Double Circuit Transmission Line	30
3.2.1	Transmission Line Tower Model	30
3.2.2	Overhead Phase Conductor & Ground Wire Model	32
3.2.3	Tower Footing Resistance Model	33
3.2.4	Insulator String Flashover Model	34
3.2.5	Double AC Source	35
3.2.6	Lightning Strike and Striking Distance	36

3.2.7	Surge Arrester	40
3.3	Lightning Attachment	41
3.4	Surge Arrester Placement	44
CHAPTER 4: RESULTS AND DISCUSSION		45
4.1	Introduction	45
4.2	Analysis of Tripping Pattern Without Surge Arresters	47
4.2.1	Lightning Current Magnitude	47
4.2.2	Tower Footing Resistance	48
4.2.3	Point Wave of AC Source Voltage	49
4.3	Analysis of Tripping Pattern With Surge arresters	50
4.3.1	Lightning Current Magnitude	51
4.3.2	Tower Footing Resistance	52
4.3.3	Point Wave of AC Source Voltage	54
4.4	Analysis of Surge Arrester Discharge Energy Capability	55
4.4.1	Lightning Current Magnitude	56
4.4.2	Tower Footing Resistance	57
4.4.3	Point Wave of AC Source Voltage	58
4.4.4	Effect of Number of Towers	61
4.4.5	Effect of Span Length	63
4.4.6	Effect of Tail Time	66
4.4.7	Effect of Front Time	68
4.5	Summary	69

CHAPTER 5: CONCLUSIONS AND RECOMMENDATIONS	70
5.1 Conclusions	70
5.2 Recommendations	71
REFERENCES	72
APPENDIX A: KKRI-GMSG LIGHTNING MAP	77
APPENDIX B: LISTS OF PUBLICATIONS	81

University of Malaya

LIST OF TABLES

	Page
Table 1 Measured lightning activity worldwide	1
Table 2.1 Parameters of the first stroke distributions adopted by Cigré	11
Table 2.2 Three types of lightning current models	19
Table 2.3 Expression for striking distance	20
Table 2.4 Tower surge impedance for different types of tower shape	22
Table 2.5 Types of tower model	23
Table 3.1 132 kV KKRI-GMSG line details	29
Table 3.2 Transmission line characteristics	33
Table 3.3 Surge arrester characteristics	41
Table 4.1 Insulator flashovers for different lightning current magnitudes	47
Table 4.2 Insulator flashovers for different tower footing resistances	49
Table 4.3 Insulator flashovers for different phase conductor angles	50
Table 4.4 Insulator flashover patterns for different lightning current magnitudes	51
Table 4.5 Insulator flashover patterns for different tower footing resistances	53
Table 4.6 Insulator flashover pattern for different power frequency angles	55
Table 4.7 Surge arrester configurations	55
Table 4.8 SA discharged energy (kJ/kV) as a function of number of tower	62
Table 4.9 Discharged energy for stroke to tower and mid span	65

LIST OF FIGURES

		Page
Figure 1.1	World keraunic map	2
Figure 2.1	Types of cloud to ground lightning discharge	8
Figure 2.2	Summary of modes of failure caused by a lightning strike	9
Figure 2.3	Back flashover and shielding failure flashover phenomena	10
Figure 2.4	Definition of the short stroke current	16
Figure 2.5	Determining parameters for impulse wave expressed in eq. (2.2)	17
Figure 2.6	CIGRE lightning current waveform	18
Figure 2.7	Geometric model, definition of angle and distance	21
Figure 3.1	Tower configuration model	30
Figure 3.2	Simple distributed line tower model	31
Figure 3.3	132 kV test system diagram	33
Figure 3.4	Insulator string flashover model	35
Figure 3.5	Power frequency voltages as a function of phase angle	35
Figure 3.6	AC voltage source window	36
Figure 3.7	Lightning current model	38
Figure 3.8	Conceptual diagram of lightning stroke to transmission line based on EGM	39
Figure 3.9	IEEE surge arrester circuit model	41
Figure 3.10	132 kV test system with lightning attachment model	43
Figure 3.11	Surge arrester connection	44
Figure 4.1	Voltage drop at double circuit line	46
Figure 4.2	Discharge energy of surge arrester	46

Figure 4.3	Power frequency voltage as a function of phase angle 100°, 180° and 220°	48
Figure 4.4	SA discharge energy as a function of lightning current magnitude	56
Figure 4.5	Power frequency voltage as a function of phase angle 60°, 100° and 240°	57
Figure 4.6	SA discharge energy as a function of tower footing resistance	58
Figure 4.7	SA discharge energy as a function of phase conductor angle	59
Figure 4.8	Discharge energy of SA at different phases as a function of phase conductor angle	60
Figure 4.9	SA discharged energy as a function of span length	63
Figure 4.10	SA discharged energy as a function of tail time	66
Figure 4.11	Lightning current waveform for different tail time	67
Figure 4.12	SA discharged energy as a function of rise time	68

LIST OF ABBREVIATIONS

AC	Alternating circuit
BFR	Back flashover rate
BIL	Basic lightning impulse insulation level
ĐT	Double circuit tripping
EGM	Electro geometric model
EMTP	Electro Magnetic Transient Program
KKRI-GSMG	Kuala Krai – Gua Musang
LDS	Lightning Detection System
MCOV	Maximum Continuous Operating Voltage
ŃT	No tripping
SA	Surge Arrester
ŠT	Single circuit tripping
TNB	Tenaga Nasional Berhad
i_A	Arrester discharge current
$i_0(t)$	Instantaneous lightning current
E_A	Arrester discharge voltage
I_m	Maximum lightning current
I_0	Lightning current peak
R_f	Simple footing resistance
R_i	Impulse footing resistance
W_A	Arrester discharged energy
Z	Tower surge impedance
τ	Time constant

CHAPTER 1

INTRODUCTION

1.1 Introduction

In general, overvoltage in the overhead line transmission systems is mainly due to the lightning strikes. Lightning is a natural phenomenon that can be considered as an atmospheric discharge of electricity, which typically occurs during thunderstorms. Malaysia, as a tropical climate country, is situated in one of the highest keraunic region, where 180 to 260 thunderstorm days per year are recorded as depicted in Table 1. Figure 1 represents the world map of keraunic level, where Malaysia lies near the equator, resulting in higher incidence of lightning activities.

Table 1: Measured lightning activity worldwide (Azizan, 2010)

Country	Thunderstorm Days Per Year Worldwide
Bogor, Indonesia (1988)	322
Cerromatoso, Columbia	275-320
Malaysia	180-260
Singapore	160-220
Florida, U.S.	90-110
Colorado, U.S.	65-100
Brazil	40-200
Argentina	30-200
Japan	35-50
Most of Europe	15-40
Australia	10-70
England	5-10

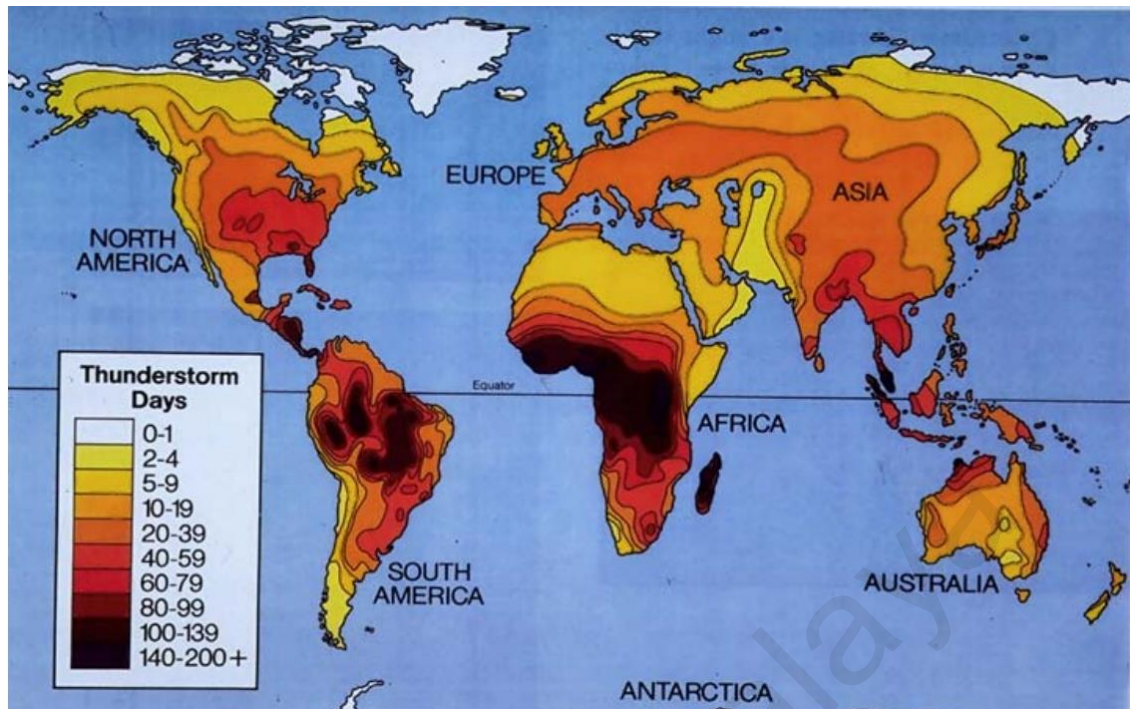


Figure 1: World keraunic map ("World Lightning Map," 2014)

Lightning can generate overvoltages when it hits either the line conductors (direct strokes) or a point in the vicinity of the overhead line transmission networks (indirect strokes). Overvoltage that occurs on the lines may cause damages to other equipment connected to the faulty line, such as substation transformers.

Lightning can damage power equipment in two ways. The first way is when the voltage across an apparatus rises the by lightning results spark over at the terminals across the struck apparatus, causing the system short circuit or the voltage penetrate through the electrical insulation of the apparatus, causing permanent damage. Another way is the lightning stroke energy may exceed the apparatus energy handling capability which will cause meltdown or fracture (Chowdhuri, 2001).

Lightning performance estimation depends on how often an overhead transmission line is struck by the lightning. In view of that, lightning activities in the region shall initially

be determined and characterized. Lightning performance of transmission line relies on the ground flash density of the region and occurrence of lightning strikes towards the line. Table 1 and Figure 1 show that Malaysia has a very high isokeraunic level and thunderstorm days per year. This lightning activity has led to multiple lines tripping on 132kV transmission lines which has been constructed, operated and maintained by the utility company.

Since lightning cannot be prevented, it is essential to understand its phenomena and characteristic so that one could intercept and divert its path through well-designed and constructed protection systems to prevent damages. There are several lightning protection solutions implemented to improve efficiency and reliability of the lines, which include earthing design enhancement, reduction of tower footing resistance and installation of ground wires. However, these protective approaches are not very effective in minimizing the effect of lightning overvoltage on the transmission lines. Installation of line surge arrester is more efficient than the other conventional methods in term of capability to reduce lightning-caused outages.

1.2 Problem Statement

Study on reliability and stability of a surge arrester during normal operation and transient over voltages are normally conducted by manufacturers and design engineers. Previous researchers have studied on the electrical parameters design and optimal placement of surge arrester based on back flashover and shielding failure rate. Few researches were conducted for arrester energy studies. Arrester energy is an important element that specifies the rating of the arrester. The energy is affected by various parameters around the transmission lines. Hence, it is crucial to conduct a thorough

study to gather information related to line surge arrester characteristics in order to select the most appropriate model, which is capable of withstanding lightning discharged energy caused by overvoltage. Proper selection and placement of line surge arresters may significantly result in optimum lightning protection by providing a compromise between the protective levels, temporary overvoltage (TOV) and energy absorption capability.

1.3 Thesis Objectives

Considering the importance of lightning protection to minimizing double circuit outages and surge arrester physical properties during transient overvoltages, the objectives of this thesis are:

1. To analyse the tripping patterns on a transmission line system to eliminate double circuit line tripping
2. To investigate the effect of lightning, tower and transmission line parameters on the surge arrester discharged energy
3. To identify the most suitable arrester placement based on the arrester discharged energy which can reduce double circuit line tripping

1.4 Contributions of the Thesis

In this thesis, 132 kV overhead transmission line were modelled using EMTP-RV software to determine the tripping patterns with and without line surge arrester for different lightning current magnitudes, tower footing resistance and point on wave of AC source voltage. The tripping patterns were determined as the phase conductor's voltage drop to zero (flashover) when the lightning current is injected at the tower top or

ground wire. Using the tripping patterns analysis, six different surge arrester configurations installed at the transmission line were proposed to study their competency to eliminate double circuit tripping and provide the maximum energy absorption that is complying with the TNB's design requirement surge arrester rating which is 5.1 kJ/kV. The surge arrester configurations were then tested for various parameters such as lightning current magnitude, tower footing resistance, point on wave of AC source voltage, number of tower, lightning tail time, lightning front time and span length to study the surge arrester discharge energy. The work conducted may enhance the understanding of tripping pattern and surge arrester discharged energy to the various transmission line parameters. Hence, the best surge arrester configuration in 132 kV transmission line can be identified.

1.5 Organization of the Thesis

This section provides a summary of all the chapters in this thesis. The overall report consists of five chapters, as follows:

Chapter 1 is the Introduction, which presents the research introduction, problem statement, objective of the research and scope of the study. The objective of the proposed method is addressed in order to outline justifications of this thesis. The contributions of the study are specified.

Chapter 2 is the Literature Review, which includes the review of publications or written materials related to the lightning overvoltage in power system networks. It provides background information on lightning strike phenomenon, back flashover event, shielding failure flashover event, surge arrester and factors that influence flashover for

lightning performance improvement. In addition, previous studies from various researchers on related topics for the thesis are also described.

Chapter 3 is the Research Methodology, which provides the methods and procedures used to achieve the objectives of this project. The main method is modelling of double circuit 132kV transmission line and towers using EMTP-RV software. It includes modelling of various components, such as transmission towers, double circuit lines, lightning current, insulator string flashover model, tower footing resistance and surge arrester. The procedure for lightning attachment and surge arrester installation are presented in this chapter to study the lightning tripping pattern and surge arrester discharge energy.

Chapter 4 is the Results and Discussion, which presents the findings of the project using EMTP-RV software. The results of the lightning tripping patterns with and without surge arresters due to certain parameters are discussed. Six different surge arrester configurations were suggested to achieve the most suitable surge arrester placement based on the lightning tripping pattern and surge arrester discharged energy. The effect of various parameters to the surge arrester discharge energy are analysed and the results are discussed at the end of this chapter.

Chapter 5 is the Conclusions and Recommendations, which concludes all findings obtained from this work. In addition, possible future work to improve the study is also listed.

CHAPTER 2

LITERATURE REVIEW

2.1 Introduction

Lightning is a visible discharge of static electricity between ground and cloud, between clouds or within a cloud. It has been one of the problems for insulation design of power systems and it is still the main cause of transmission and distribution lines outages. Malaysia, having a very high number of lightning days per year, at 220 days per year and recorded flash density of 20 flashes/km/year typically experiences overvoltages due to lightning strikes (Bakar, Talib, Mokhlis, & Illias, 2013). Transmission line faults due to lightning strikes cause serious damages, such as massive blackout and instantaneous voltage drop on electric power systems (You, Zhang, Cheng, Bo, & Klimek, 2010).

Generally, flashes that lower positive charges to ground are specified as positive lightning, while those that transfer negative charges to ground are referred to negative lightning. Due to their initiating leader process, they are further classified into upward and downward lightning.

Downward lightning is characterised into two types. The positive downward lightning has a positive downward leader, while the negative downward lightning has a negative downward leader, as depicted in Figures 2.1(a) and (b). This leader is propagating down from the thundercloud towards ground to discharge lightning. Structures or buildings up to about 100 m are often struck by this type of lightning.

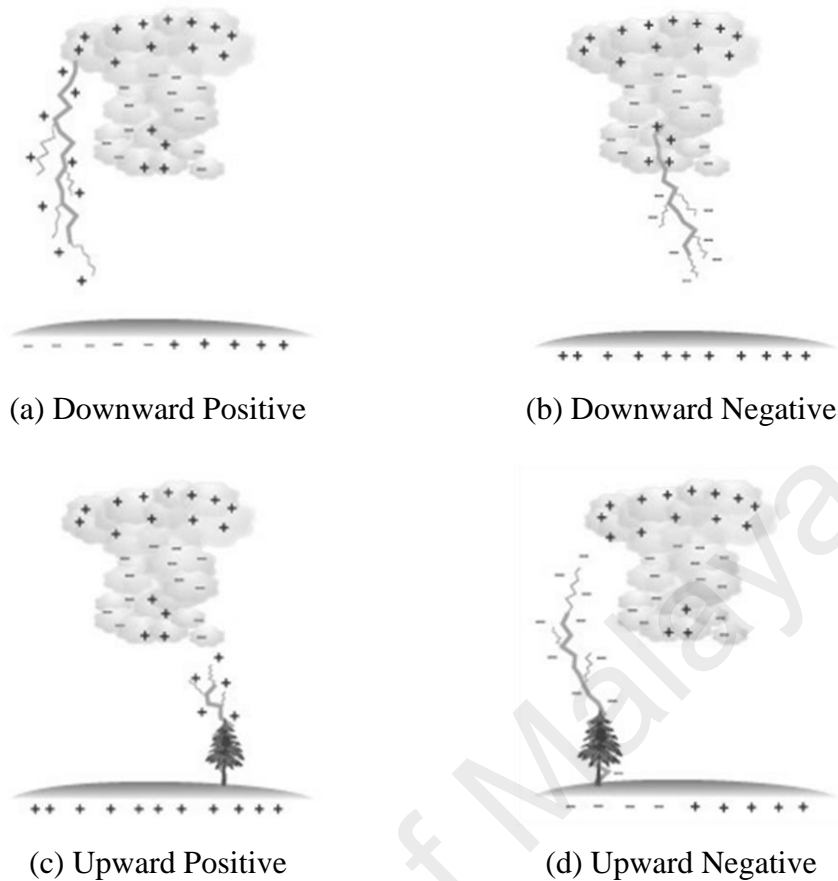


Figure 2.1: Types of cloud to ground lightning discharge (Uman, 2001)

When the downward propagating leader approaches ground, the electric field at grounded objects increases due to the charge contained in the downward leader channel. As soon as the electric field exceeds a certain level, connecting leaders start from the grounded objects, making the final connection between the objects at ground and the downward leader. This is the beginning of the return stroke phase, where the return stroke current flows through the struck object.

Figures 2(c) and (d) show another type of lightning discharge, which is upward lightning for positive and negative upward leaders. For this type of lightning, the leader initiates from the top of the structure or building and increases the electric field. To exceed the critical electric field strength, the structure or building must have a height of about 100 m at minimum.

2.2 Lightning Phenomena at Transmission Lines

Lightning flashovers at transmission lines are divided into three types; lightning that strike on a phase conductor, on an overhead ground wire, or to nearby ground (CIGRE WG 33-01, 1991). Figure 2.2 shows the summary of transmission line failures caused by lightning strikes. Flashover that occurs from the lightning strike to ground wire is called back flashover while for lightning strike directly to phase conductor is called shielding failure flashover.

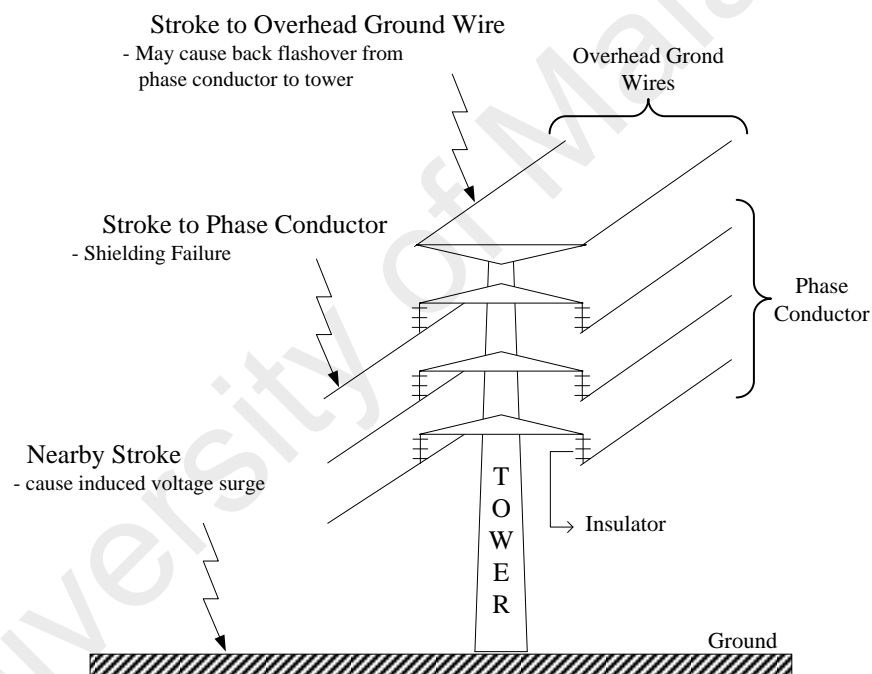


Figure 2.2: Summary of modes of failure caused by a lightning strike

2.2.1 Back Flashover Event

Back flashover is the most common lightning transient problems which causes surge on transmission line systems (IEEE Std 1243-1997, 1997). The event occurs when ground systems, which are ground wires, tower tops, and pole tops is hit by a lightning (A), as shown in Figure 2.3. A lightning current will flow to the adjacent tower via the ground

wire (1 and 2). Another part of the resulting travelling wave travels down the tower via the tower body (3). The effective surge impedance of the tower will cause the travelling wave to be reflected to the tower top and the phase conductors, thus, increasing the induced voltage.

The voltage difference between the phase conductor and the cross arm must exceed the line critical flashover voltage (CFO) in order to cause flashover (5) from the tower back to the conductor. The phase with the poorest coupling to the ground wire will be the most highly stressed and therefore most likely flashover will occur. Local grounding conditions have a major impact on the back flashover performance. This phenomenon is referred as back flashover since it is in the opposite direction of flashovers obtained from experimental studies.

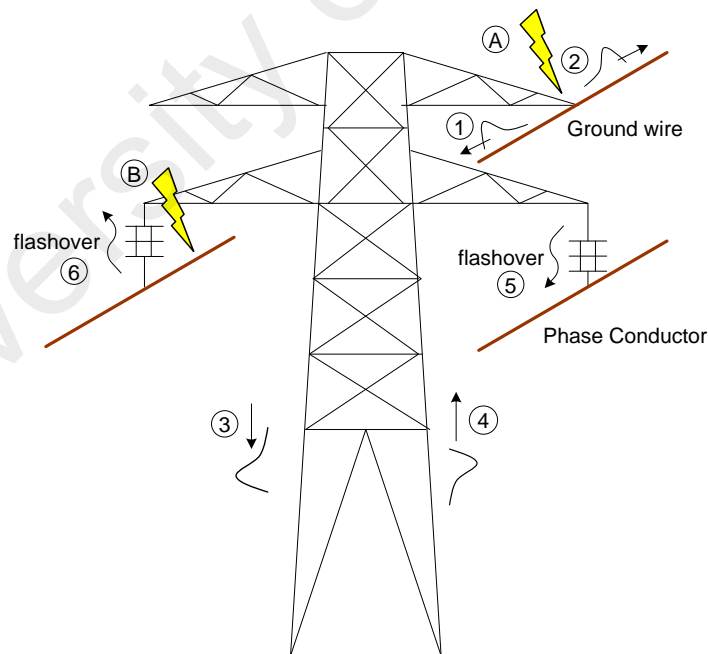


Figure 2.3: Back flashover and shielding failure flashover phenomena

2.2.2 Shielding Failure Flashover Event

Referring to Figure 2.3, shielding failure flashover events (6) results from a lightning stroke misses the ground wire and terminating directly on a phase conductor (B) (Nucci, 2009). For shielded lines, these events should be very infrequent and of very low stroke current magnitude. For unshielded lines that are staticless lines, these events will be much more common and will involve the full distribution of lightning stroke current magnitudes. The significant parameters of the current stroke, which contributes to both phenomena, are stated in Table 2.1 ("IEEE Guide for the Application of Insulation Coordination," 1999). Shielding failure occurs when lightning current is below 20 kA, while back flashover occurs when lightning current is higher than 20 kA.

Table 2.1: Parameters of the first stroke distributions adopted by Cigré (Nucci, 2009)

Parameter of (I)	Shielding failure domain $I < 20$ kA	Back flashover domain $I > 20$ kA
Median value (kA)	61	33.3
Logarithmic standard deviation	1.33	0.605

To encounter these problems, several lightning protection system were introduced (IEEE Std 1243-1997, 1997; Xi, Li, & He, 2014). The lightning protection system is introduced to diminish the probability of a direct lightning strike to the transmission lines and tower. A lightning protection system does not prevent lightning from striking but it control and prevent the damage by providing a low resistance path for the lightning discharge energy.

2.3 Lightning Surge Analysis Methods on Transmission Lines

Improving lightning performance on transmission lines is crucial to avoid physical damage to the system equipment, which may result in service interruption to the electricity consumers. Several studies have been conducted to analyse the lightning surge at transmission lines to improve the efficiency and reliability of the transmission lines (Bakar et al., 2013; Christodoulou, Ekonomou, Mitropoulou, Vita, & Stathopoulos, 2010; Hayashi, Mizuno, & Naito, 2008; Malcolm & Aggarwal, 2014; Pinto et al., 2014; Tarasiewicz, Rimmer, & Morched, 2000)

2.3.1 Field Data

Most researchers used field data to conduct lightning studies on the overhead transmission lines (Taniguchi et al., 2010; Rawi & Ab Kadir, 2014). It is crucial to study the real data of line system and event of lightning current strike to determine the correct analysis method and the accuracy of the results. Lightning stroke current data is captured using lightning monitoring system and used to evaluate and compare with the results of lightning analysis methods. In Malaysia, Lightning Detection System Lab (LDS) operated by TNB Research Sdn. Bhd. is installed to monitor the lightning performance of overhead transmission lines in peninsula Malaysia. These data are used in the lightning analysis method studies. By studying the real incident on specific transmission lines, correct mitigation or improvement can be done to achieve desired lightning protection designs at specific area.

2.3.2 Back Flashover Rate

Lightning surge analysis of back flashover event at overhead transmission lines can be evaluated by using back flashover rate, BFR (Hileman, 1999; Sardi et al., 2008). BFR in terms of flashovers per 100 km-years, equals to the stroke current probability, $P(I_C)$ multiplies with the strokes number, N_L , that terminate on the overhead ground wire or tower. The number of strokes, N_L can be determined using the geometric model (Taniguchi et al., 2010). BFR is calculated using

$$BFR = 0.6N_L P(I_C) \quad (2.1)$$

where

$P(I_C)$ = probability of the lightning current stroke equals or exceeds the critical back flashover current,

N_L = strokes number that terminate on the ground wire per 100 km-year

BFR data is used to determine the Basic Lightning Impulse Insulation Level, BIL of equipment at transmission system, such that they can withstand lightning overvoltage without breakdown. Thus, proper insulation coordination scheme can be created to improve the lightning line performance at transmission system. C++, TFlash and Sigma-Slp are the software usually used by researchers to perform this method.

2.3.3 Simulation Method

It is hard to physically observe lightning surge overvoltage occurrences at transmission lines. Furthermore, to run experiments related to lightning is expensive and risky as most of the equipment is in high voltage rating. Thus, simulation is the best option to

investigate the lightning effect on transmission lines. Many simulation software have been used to study the behavior of lightning flashover, such as ATP, EMTP and PSCAD software (Gouda, El Dein, & Amer, 2010; Saengsirwan & Thipprasert, 2004; J Sardi & Chian, 2010). The basic configuration of model system that has been recommended for lightning surge simulation includes the overhead transmission lines, transmission tower, tower footing resistance, insulator flashover model and the lightning current model (Ishii & Kawamura, 2011; Munukutla, Vittal, Heydt, Chipman, & Keel, 2010). Most of the parameters of the model are taken from the field data to investigate the real event.

Thin H. Pham have analysed the result of externally gapped line arrester (EGLA) placement on the lightning performance on a double circuit 220 kV transmission line (Pham et al., 2012). The numbers of EGLAs installed on the transmission line were varied from 1 to 3 to estimate the effectiveness of EGLA. Three possible EGLAs placement were studied by varying the lightning current and footing resistance parameters. Installing EGLAs with suitable rating on all phases of one circuit reduces the possibility of a double circuit tripping for lightning to tower top. However, insulator flashover on the unprotected parallel circuit still occurs for very high footing resistance and lightning current.

2.4. Factors Affecting Flashover Patterns

Lightning which strikes the ground wire of a transmission line can result in different patterns of flashover on phase conductors. The patterns depend on many factors, which include the type of transmission line, lightning current parameter, characteristics of transmission tower, tower footing resistance and insulator string.

2.4.1. Line Parameters

Generally, there are three types of transmission line models: Bergeron model (Constant-Parameter Distributed Line), Frequency-Dependent model (J-Marti model) and PI-model (Bergeron, 2009; Marti, 1982; Martinez, Gustavsen, & Durbak, 2005). The PI-model is a frequency-independent and lumped model. It is suitable for medium lines. Bergeron model consists of discrete inductance and capacitance parameters, which is similar to a combination of numberless PI-model. The model represents the fundamental frequency for a constant value of surge impedance. It is also more precise compared to the PI section model, especially when designing a transmission line where travelling wave time is longer than the simulation time step. The frequency-dependent model can precisely describe the transient travelling wave propagation process in a wider frequency range due to its parameters vary with the frequency. However, the model is more suitable to be used for systems of ideally transposed conductors (Ametani & Kawamura, 2005; Dommel, 1986).

2.4.2. Lightning Current Parameters

Lightning current is one of the important parameters in studying the performance of transmission line due to lightning. There are three types of lightning current model that are commonly used in lightning study; double exponential function, Heidler method and Cigre' method. Figure 2.4 shows the general shape of lightning wave used in the simulation, where T_1 is the front time, T_2 is the decay/tail time and $i(t)$ is the lightning current magnitude with the function of time, t . For effective shielding, it is better to determine the maximum lightning current that can be shielded by ground wire by using electro geometric model.

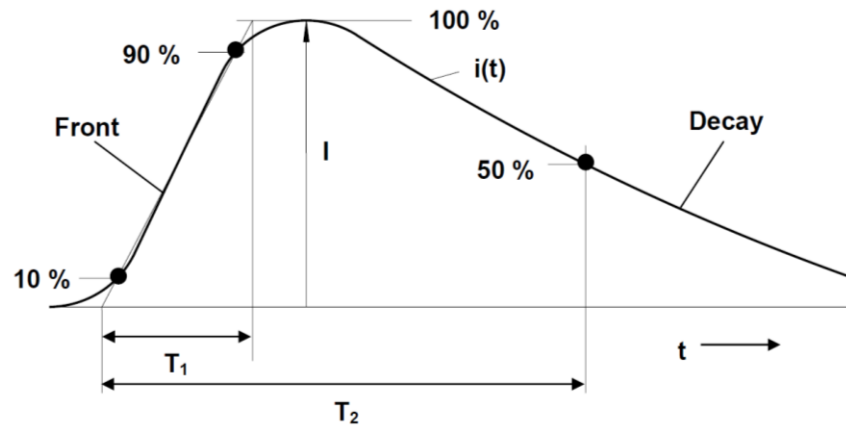


Figure 2.4: Definition of the short stroke current

A) Double Exponential Function

A simplified lightning current model, which is double exponential function, was introduced by Bruce and Golde to represent lightning stroke (Bruce & Golde, 1941).

The function is represented by

$$i_0(t) = kI_0(e^{-\alpha t} - e^{-\beta t}) \quad (2.2)$$

where

$i_0(t)$ = instantaneous lightning current

I_0 = lightning current peak

t = instantaneous time, μs

α, β = lightning current wave tail and wave head attenuation quotient

k = waveform correction index

The parameters of α and β can be obtained by referring to Figure 2.5, where a is α , b is β , t_1 is the front time, t_2 is the tail time and I is the lightning current magnitude.

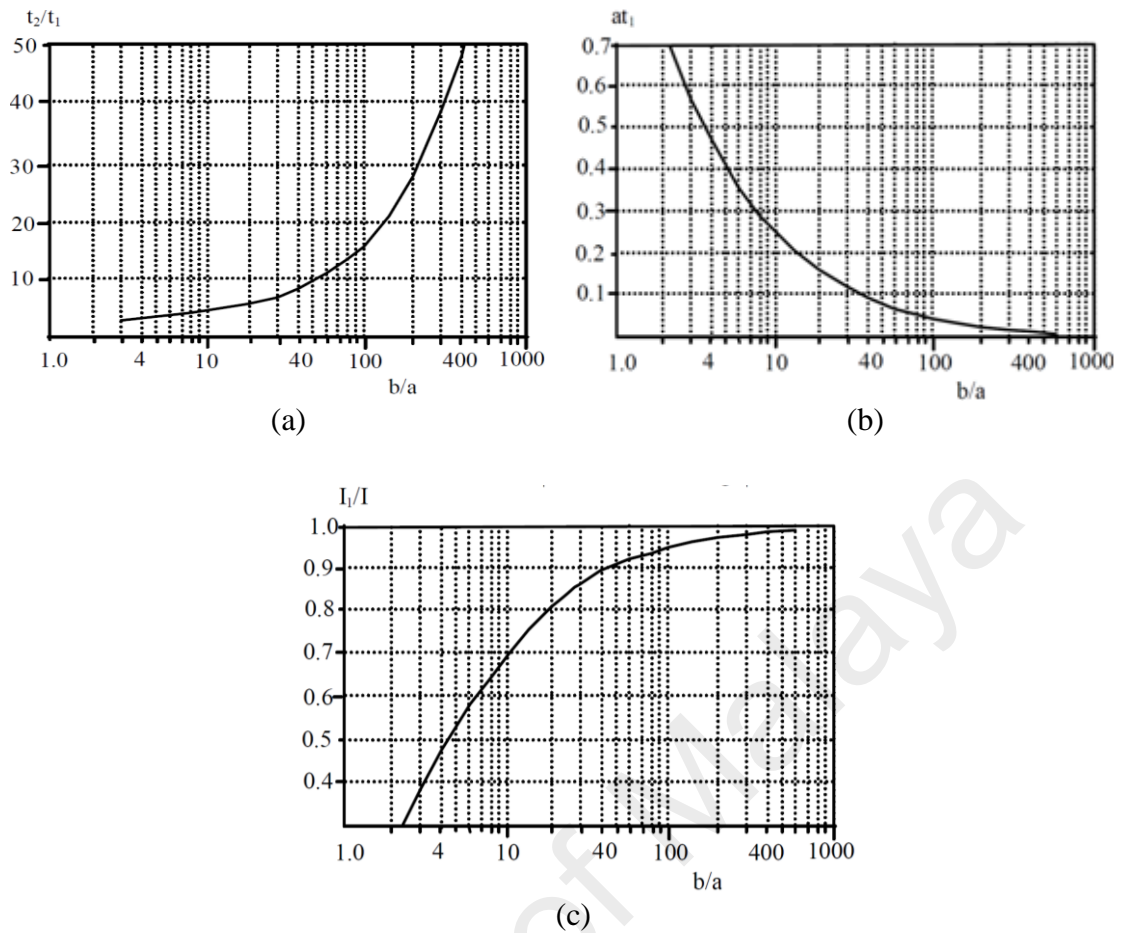


Figure 2.5: Determining parameters for impulse wave expressed in eq. (2.2)

(‘Applications of PSCAD/EMTDC’, 2007)

B) Heidler method

Heidler method is a class of analytical functions used to study the lightning effect associated with the current front (Heidler & Cvetić, 2002). Eq. (2.3) represents the simplified lightning waveform used in this model,

$$i_0(t) = I_0 \cdot k^n \cdot e^{-t/\tau_2} / \left(\eta \cdot (1 + k^n) \right) \quad (2.3)$$

where

η = the peak current correction factor, < 1

n = current steepness factor, > 1

$$k = t / \tau_l$$

$$\tau_l = \text{tail time} / \ln 2, \text{ time constant}$$

$$\tau_l = \text{front time} / \ln 2, \text{ time constant}$$

C) Cigre method

The concave shape waveform as recommended by CIGRE provides a more accurate and realistic representation of the concave front of a lightning stroke (IEC TR 60071-4, 2004). The waveform characteristic that focuses on the wave front side is shown in Figure 2.6. The front parameters are described by the crest current, I_f , the maximum rate of rise, S_m , time when 90% of crest current, t_n and the equivalent front time duration, t_f , respectively.

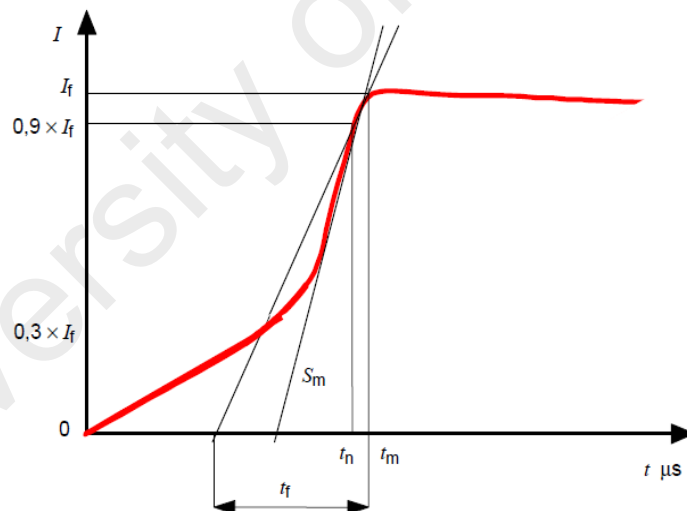


Figure 2.6: CIGRE lightning current waveform (CIGRE WG 33-01, 1991)

The differences between the three current models are the front wave shape and the time when the lightning peak occurs. This dissimilarity may cause different results in the simulation. Table 2.2 shows the difference between the three types of lightning current models.

Table 2.2: Three types of lightning current models

Lightning current model	Figures
Double exponential function	
Heidler method	
Cigre' method	

D) Electro geometric model

The geometric model of the last lightning stroke step was introduced and used to determine the number of flashes to the ground wires. Considering the general concept as depicted in Figure 2.7, for a specific value of stroke current, arcs of radii r_c are drawn from the phase conductors and from the ground wires. A horizontal line of distance r_g

from the earth surface is constructed. The intersections between these arcs and the intersection of the arcs with the horizontal line are marked as A, B, and C. Downward leaders that reach the arc between A and B will be terminating on the phase conductor. Those reach the arc between B and C will be terminating on the ground wires, and those terminate beyond A will be terminating to ground or earth. Table 2.3 shows the expression for the striking distance, r (Eq. 2.4), which was validated by different sources. The shielding angle, α , as shown in Figure 2.7 also plays an important role in shielding the transmission line. Shielding angle should be kept at 30 degree or less-angle measured from the vertical between the ground wire and phase conductor (Hileman, 1999). Eq. (2.4) is the distance from a grounded structure to the leader tip when a connecting leader is initiated from the structure, which is transmission line tower.

$$r = AI^b \quad (2.4)$$

Table 2.3: Expression for striking distance (Hileman, 1999)

Source	r_g to earth / ground		r_c to phase conductors & ground wires	
	A	b	A	b
Wagner (Wagner & Hileman, 1961)	14.2	0.42	14.2	0.42
Armstrong & Whitehead (Armstrong & Whitehead, 1968)	6.0	0.8	6.7	0.8
Brown & Whitehead (Brown & Whitehead, 1969)	6.4	0.75	7.1	0.75
Love (Love, 1973)	10.0	0.65	10.0	0.65

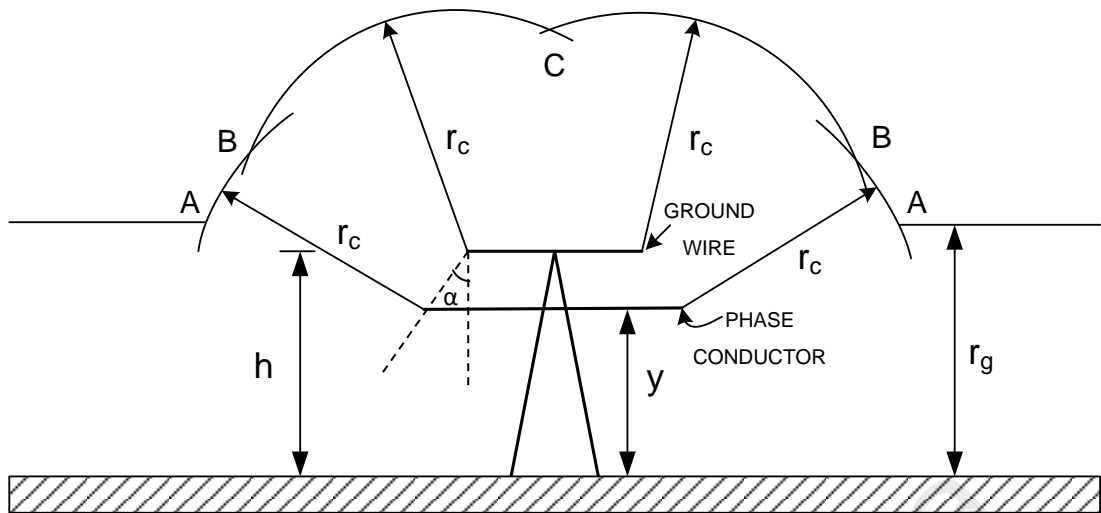


Figure 2.7: Geometric model, definition of angle and distance (Hileman, 1999)

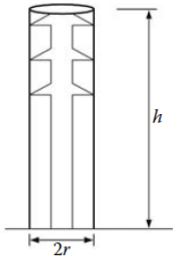
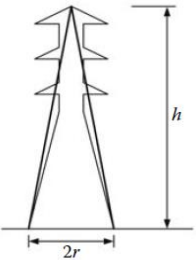
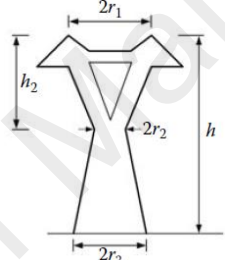
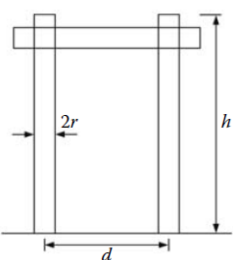
2.4.3 Transmission Tower Parameters

Parameters of transmission tower that affect the patterns of flashover on phase conductors are the tower surge impedance and tower configuration.

A) Tower Surge Impedance

Various tower surge impedance equations have been proposed from previous studies on overhead transmission line modelling (Martinez-Velasco, 2010). Table 2.4 shows the tower surge impedance for different types of tower shape, where c is the speed of light (IEEE Working Group, 1985; IEEE Std 1243-1997, 1997; Whitehead et al., 1993). The equation is an approximation since the tower surge impedance is a time varying quantity. However, the formula is easy to be applied and results in close agreement with the measured results of tower surge impedance.

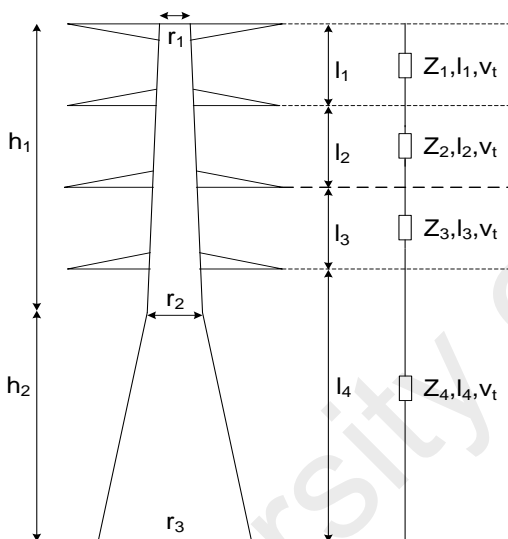
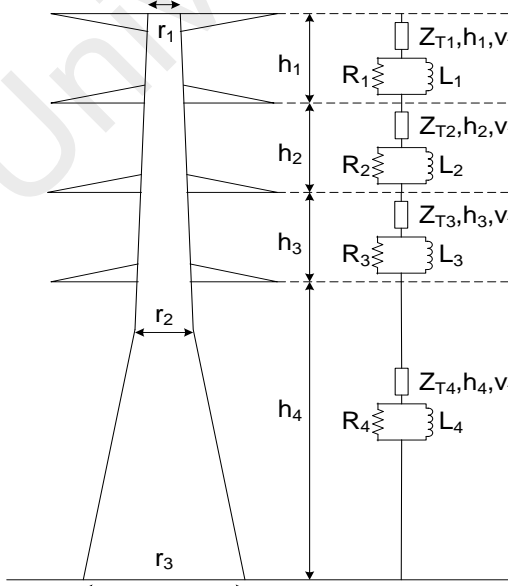
Table 2.4: Tower surge impedance for different types of tower shape

Tower Wave Shape	Cylindrical	Conical	Waist	H-frame
Figure				
Surge Impedance	$Z = 60 \left(\ln \left(2\sqrt{2} \frac{h}{r} \right) - 1 \right)$	$Z = 60 \ln \left(\sqrt{2} \sqrt{\left(\frac{h}{r} \right)^2 + 1} \right)$	$Z = \sqrt{\frac{\pi}{4}} 60 \left(\ln \left(\cot \frac{\tan^{-1}(r/h)}{2} \right) - \ln \sqrt{2} \right)$ $(h=h_1+h_2)$	$Z_1 = 60 \left(\ln \left(2\sqrt{2} \frac{h}{r} \right) - 60 \right)$ $Z_2 = \frac{d \cdot 60 \ln \left(2 \frac{h}{r} \right) + (h \times Z_1)}{h + d}$ $Z = \frac{Z_1 \times Z_2}{Z_1 + Z_2}$
Travel time	$t = \frac{h}{0.85 \times c}$	$t = \frac{h}{c}$	$t = \frac{h}{0.85 \times c}$	$t = \frac{1}{c \times Z} \frac{h \times Z_1 (d + h) \times Z_2}{h \times Z_1 + (d + h) \times Z_2}$

B) Tower Model Configuration

Table 2.5 shows two types of tower model that are frequently used in transmission line studies. The simple distributed line tower model is suitable for tower height less than 30 m (Sadovic & Sadovic, 2009) while for higher tower, multi-storey tower model are commonly used.

Table 2.5: Types of tower model

Tower model	Model parameter
<p style="text-align: center;">Simple distributed line model</p> 	$Z_t = 60 \left[\ln(h/R) - 1 \right]$ $R = \frac{r_1 h_1 + r_2 h + r_3 h_2}{2h}$ <p>where R = equivalent radius of the tower h_1 = height from top to midsection, m h_2 = height from midsection to base, m $h = h_1 + h_2$ r_1, r_2, r_3 = radii of tower top, midsection and base, m</p>
<p style="text-align: center;">Multi-storey tower model</p> 	<p>Assuming that $Z_{T1} = Z_{T2}$. Z_{T1} is calculated using Jordan's formula by</p> $Z_{T1} = Z_{T2} = 60 \left[\ln(h/R) - 1 \right]$ <p>R is calculated using the same model as Simple distributed line model parameter</p> $R_i = \frac{-2 \cdot Z_{T1} \cdot \ln \sqrt{\gamma} h_i}{h_1 + h_2 + h_3}$ $R_4 = -2 \cdot Z_{T2} \cdot \ln \sqrt{\gamma}$ $L_i = \alpha \cdot R_i \cdot 2h/c \quad (i = 1, 2, 3, 4)$ <p>where h = each tower section height γ = attenuation coefficient (0.7 - 0.8) α = damping coefficient (unity)</p>

2.4.4 Tower Footing Resistance

Tower footing resistance is one of the most important parameters in determining the transmission line performance. Since voltage and current reflection and refraction coefficients are the functions of footing resistance, the selection of the footing resistance will determine the performance of a transmission line. Under fast front transient events, the resistance value is normally less than the measured one at low frequencies. This is due to a significant ground current that causes sufficient voltage gradients to break down the soil around the ground rod. The footing resistance varies for different type of soil. High footing resistance is commonly found on rocky terrains. The most common tower footing resistance representations are simple linear resistance and nonlinear resistance (Ametani & Kawamura, 2005; Gazzana et al., 2014; IEEE Working Group, 1985; Whitehead et al., 1993).

2.4.5 Insulator String

The type of the insulator string used will determine the value of critical flashover rate, (CFO), which can affect the occurrences of flashover at a transmission line. The induced voltage flashover events resulting from the nearby lightning strokes will induce voltage on line conductors. Since the induced overvoltage measured on the distribution lines rarely exceeds 300 kV, it is common that this phenomenon has little effect on transmission voltage levels. However, the induced voltage tends to increase with the height of the line. Insulator strings made of high dielectric strength material can reduce the number of flashovers at the transmission line due to the high voltage withstand capability (Hileman, 1999).

2.5 Protection of Transmission Lines

In order to ensure the continuity of supply to consumer, several protection methods have been introduced to improve the lightning performance (CIGRE WG 33-01, October, 1991; Hileman, 1999; IEEE Std 1243-1997, 1997). They include adding ground wires, reducing tower footing resistance, increasing the insulation and installing line surge arresters.

2.5.1 Surge Arrester

Line surge arrester is a device installed on transmission lines of a power system network to reduce the probability of flashover during lightning and switching surge events. The protective device, which is usually installed between the phase conductor and earth acts as insulation during normal operating conditions. The arrester main functions are to divert the lightning to the ground, clamp the voltage induced by the lightning before returning to its original state and only protects equipment electrically parallel with it. The arrester develops a discharge voltage across its terminal, which is a function of the magnitude and wave shape of the discharge current wave, arrester design and voltage rating. After the lightning surge current has been discharged, a correctly installed surge arrester is capable to repeat its protective function until another surge voltage has to be discharged.

It is important to understand the behaviour of the surge arrester when it is stressed by overvoltage with different wave shapes and amplitudes. Various studies have been conducted to determine the best location and placement of the arrester to minimise system momentary outage (Woodworth, 2009). The arrester must be installed at every

tower or pole to be effective at preventing shielding failure flashovers. The use of surge arresters in lightning protection of overhead transmission lines is to improve reliability of electric utilities. However due to the economic reasons, it is not possible to install surge arresters at each transmission structure of overhead transmission line. Hence, proper selection of surge arrester placement can provide the optimum solution to major lightning problems and result in economical installation cost.

2.5.2 Arrester Discharge Energy

Surge arrester energy handling capability is one of the important factors in specifying and selecting suitable type of an arrester to be installed. The arrester must be capable of withstanding discharge energy to eliminate lightning surges. The protective device must not exceed two types of energy absorption limit, which are (Woodworth, 2008):

a) Thermal Energy Absorption Limit

This limit is the maximum level of energy that can be injected into an arrester at which it can return to its normal operating temperature while being energized.

b) Single Impulse Energy Absorption Limit

This limit is the maximum value and duration of energy injection required to damage an arrester permanently at both macroscopic and microscopic level.

To develop the equation for the arrester energy during back flashover event, the following expression is used (Hileman,1999),

$$W_A = E_A i_A \tau \quad (2.5)$$

where

W_A – arrester discharged energy, kJ

E_A – arrester discharge voltage, kV

i_A – arrester discharge current, kA

τ – time constant, μs

University of Malaya

CHAPTER 3

RESEARCH METHODOLOGY

3.1 Introduction

The main objective of this work is to perform lightning transient studies to find the optimal placement of surge arresters to improve lightning performance using Electromagnetic Transient Program (EMTP) software. There are three major parts involve in the methodology of this work. The first part is to model a full system 132 kV transmission line with its accessories, lightning impulse and surge arrester. The next part is to study the behaviour of transmission line tripping patterns when lightning is injected onto the transmission line. Finally, surge arrester placement is analysed to find the optimal arrester placement for line protection.

3.1.1 Introduction of EMTP Simulation Software

Electromagnetic Transients Program (EMTP) is a powerful computer program that can be used to simulate and analyze electromagnetic, electromechanical and control systems on electric power networks. EMTP can be used successfully for various studies in real time simulation with oscillation ranging in duration from microsecond to minute. There is a standard library in the features that can contain details components and function blocks that allows creating complete and complex power system studies such as precise models of lines and cables, advanced model of electrical machines, lightning current models and many more. The software also comes with friendly interface with MATLAB software for analysis purpose.

Typical studies using EMTP are as follows:

1. Insulation coordination: overhead lines, outdoor stations etc.
2. Lightning surges: back flashover, induced surges
3. Protection: power oscillations, saturation problems, surge arrester influences
4. Transmission line system: insulation coordination, switching, design, wideband line and cable models
5. Ferro resonance
6. Switching surges: deterministic, probabilistic, single-pole switching, high-speed reclosing, capacitor switching

3.1.2 Test System

A double circuit transmission line of 132 kV Kuala Krai–Gua Musang (KKRI-GMSG) in Malaysia is chosen as the case study in this work. This is due to it has experienced the most lines tripping in the year 2001 until 2005, which is 29 recorded double-circuit trippings. The statistics of tripping events were obtained from relay readings at lightning magnitude in the range of 34 to 122kA (Appendix A). Table 3.1 shows the details of 132 kV double circuit KKRI-GMSG transmission line used in this study, which are obtained from TNB (Bakar, Othman, & Osman, 2007).

Table 3.1: 132 kV KKRI-GMSG line details

ITEM	DETAIL
Type of line	Double circuit line
Starting substation	Kuala Krai
Ending substation	Gua Musang
No. of tower	295
Line length (km)	113.2
Phase arrangement	L1 (Blue-Red-Yellow) L2 (Yellow-Blue-Red)

3.2 Modeling of Double Circuit Transmission Line

3.2.1 Transmission Line Tower Model

In this work, a 132kV double circuit with two overhead ground wire transmission line system was considered. The tower height is 28.22 m with double circuit vertical phase conductor configuration with two ground wire, as shown in Figure 3.1.

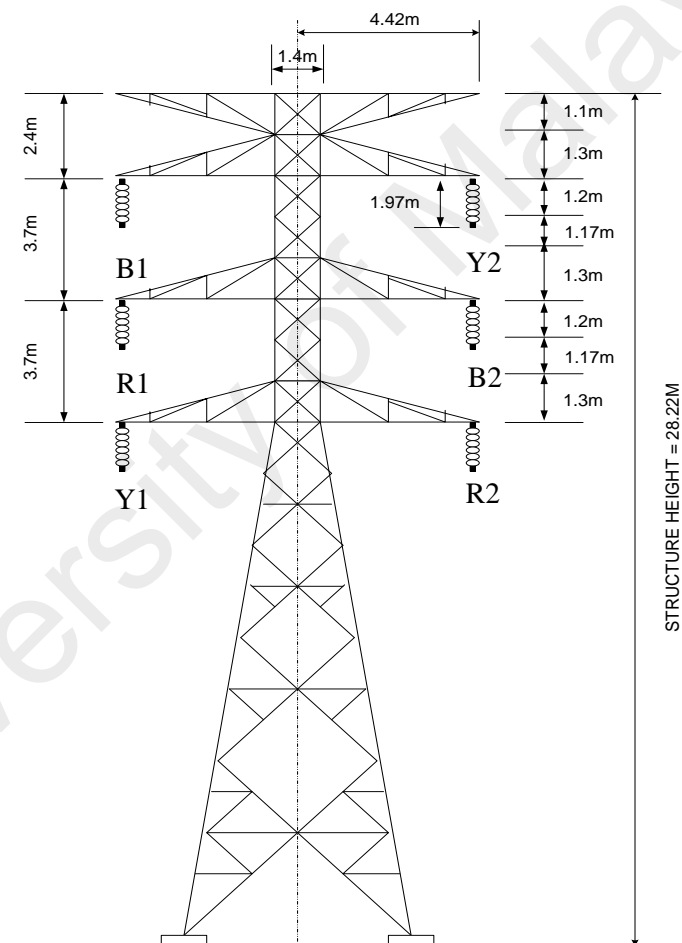


Figure 3.1: Tower configuration model

Simple distributed line model was selected to be the tower model in the simulation because it is able to provide acceptable accuracy for transmission tower of less than 500 kV (Ito, Ueda, Watanabe, Funabashi, & Ametani, 2003). Also, the simple distributed

line model is relatively simple compared to other tower models, such as multi conductor and multi storey tower model. Figure 3.2 shows the tower model in EMTP-RV. There are several equations to determine the surge impedance of the tower. For conical tower shape, the following equations are used (Ito, Ueda, Watanabe, Funabashi, & Ametani, 2003):

$$Z = 60[\ln(h/R) - 1] \quad (3.1)$$

where,

$$R = \frac{r_1 h_1 + r_2 h + r_3 h_2}{2h} \quad (3.2)$$

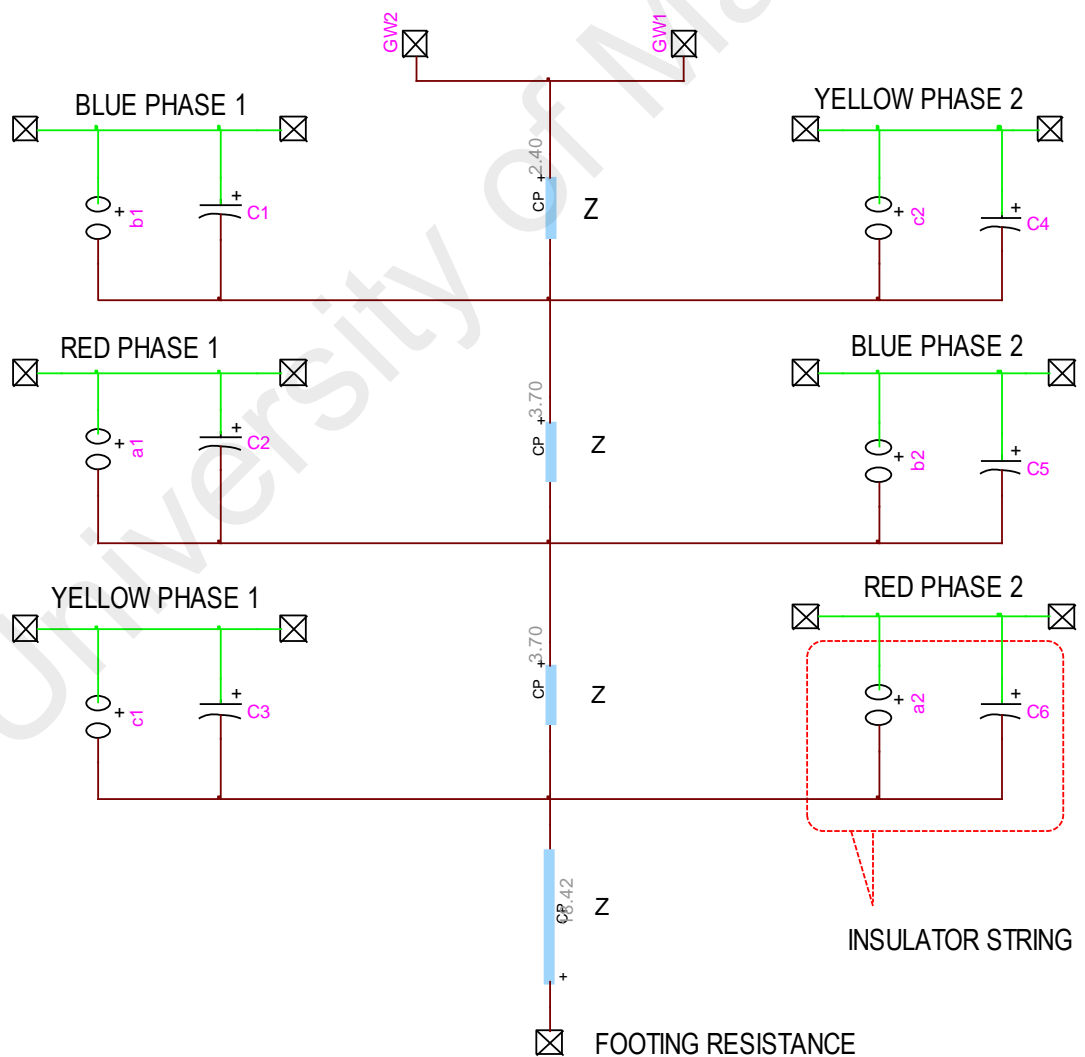


Figure 3.2: Simple distributed line tower model

R is the equivalent radius of the tower represented by a truncated cone, $h = h_1 + h_2$, and

r_1, r_2, r_3 – radii of tower top, tower midsection and tower base, m

h_1 – height from top to midsection, m

h_2 – height from midsection to base, m

3.2.2 Overhead Phase conductor and Ground wire model

Ground wire with double circuit vertical phase conductor configuration was used for 132kV Kuala Krai-Gua Musang (KKRI-GMSG) transmission line. Two ground wires are installed at the top of the tower to protect the phase conductors from direct lightning strike. The arrangement of the phase conductors at the first and second circuit is installed differently, as shown in Figure 3.1. At the first circuit, the phase conductors are arranged with blue phase at the top followed by the red and yellow phases. For the second circuit, the yellow phase conductor is installed at the top followed by the blue and red phases. The advantage of particular phasing arrangement conductor in the double circuit transmission line is improving the efficiency of power supply by reduction of the resistive losses and reduction of the electric and magnetic field in the system (Dezelak, Stumberger, & Jakl, 2010; Nourai, Keri, & Shih, 1988). The arrangement of the vertical configuration phase conductors and ground wires needs to be taken into account, as shown in Figure 3.2.

Nine transmission towers were modelled based on the actual lattice tower of 132 kV transmission line in Malaysia, which are separated by line span of 300 m, as illustrated in Figure 3.3. Nine transmission towers are used to avoid any overvoltage transient reflected back to the injection tower. The velocity of the wave propagation was assumed to be equal to the speed of light in free space, which equals to 300 m/ μ s. The

phase conductor and ground wire characteristics used in this study are shown in Table 3.2.

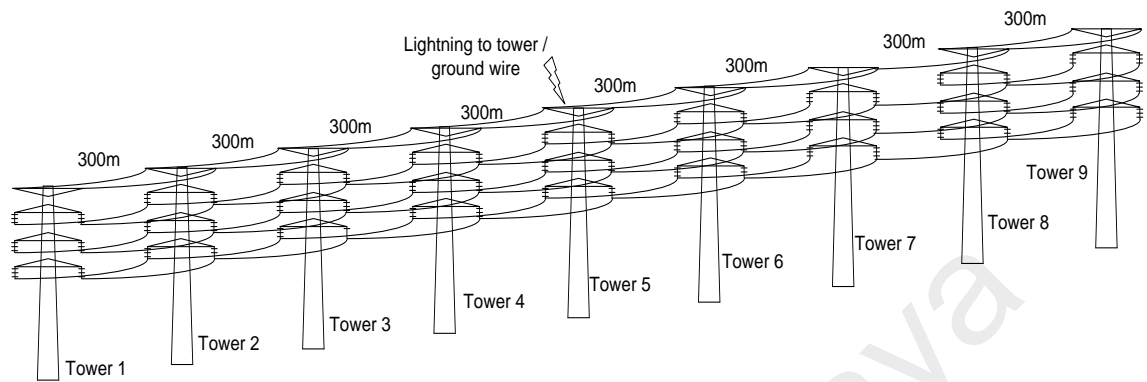


Figure 3.3: 132 kV test system diagram

Table 3.2: Transmission line characteristics

	Type	Diameter (mm)	Resistance (Ω /km)
Phase conductor	Batang	24.16	0.08914
Ground wire	OPGW	12.2	0.537

3.2.3 Tower Footing Resistance Model

The lightning performance of transmission lines is strongly related with the tower footing resistance (Talib, Bakar, & Mokhlis, 2012). The tower footing resistance, R_0 for fast transient surge or at high frequency (impulse footing resistance, R_i) is normally less than the measured value at low frequencies. This is due to a significant ground current that causes sufficient voltage gradients to breakdown the soil around the ground rod. However, in this study, a simple linear resistance, R_f is used in the model, as commonly practiced in literatures (Ametani & Kawamura, 2005; IEEE Working Group, 1985; Whitehead et al., 1993).

3.2.4 Insulator String Flashover Model

A voltage controlled switch (S), which is connected in parallel with a capacitor (C) was used to represent the insulator string, as shown in Figure 3.4. In order to predict the insulator dielectric strength when overvoltage occurs due to a lightning, three approaches can be used; voltage-time curves, integration method and leader progression model (Martinez-Velasco, 2010). However, the integration method was used to determine the dielectric strength of the insulator string due to its simplicity. Using this method, several assumptions have been made, they are; the minimum voltage, V_0 must be exceeded before a breakdown can occur and for each configuration of an insulator, there is a set of constants associated with the breakdown. The disruptive effect constant, D , is calculated based on equation (3.3) and equation (3.4) to determine the dielectric breakdown of the insulation (Darveniza, 1988),

$$\int_{t_0}^{t_1} (|V_{gap}(t)| - V_0)^k dt \geq D, \quad k = 1 \quad (3.3)$$

$$V_0 = 0.9V_{50\%} = 0.9(400 + (710/t^{0.75}))d \quad (3.4)$$

where $V_{gap}(t)$ is the voltage across the insulator string, kV; $V_{50\%}$ is the 50% breakdown voltage, kV; V_0 is the minimum voltage, kV; t_0 is the time after which the voltage $V_{gap}(t)$ is higher than the required minimum voltage V_0 , μ s; t_1 is the elapsed time after lightning strike, μ s; t is the tail time of the lightning current waveform, μ s and d is the insulator length, m. From the equations, $D = 0.1308d$. Therefore the parameters of V_0 and D used in the integration method for the 132 kV line are 975.15 kV and 0.2576.

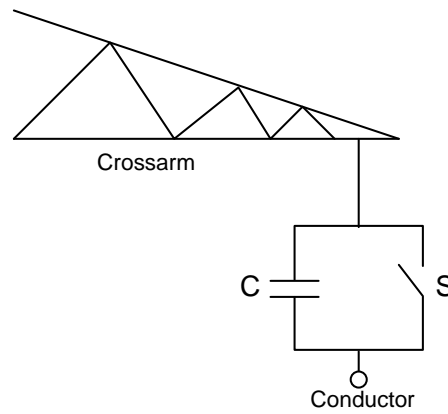


Figure 3.4: Insulator string flashover model

3.2.5 Double AC Source

The double circuit transmission line can carry two supplies of electricity at the same time. In this work, two separate AC source were used, as illustrated in Figure 3.5. Both sources are set to be synchronous with each other where the red, blue and yellow phase supplies for each circuit run at the same phase degree, time and voltage magnitude (Figure 3.6).

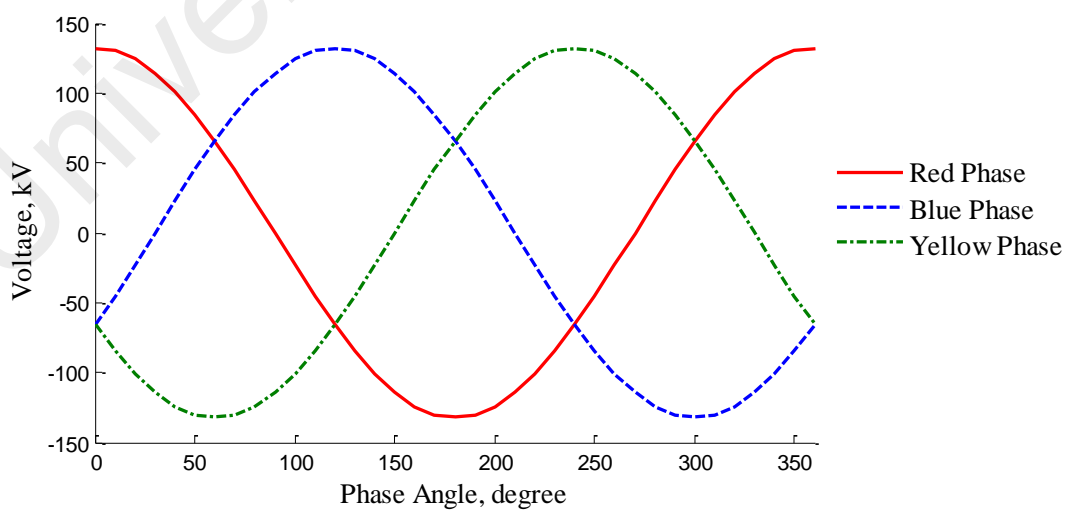


Figure 3.5: Power frequency voltages as a function of phase angle

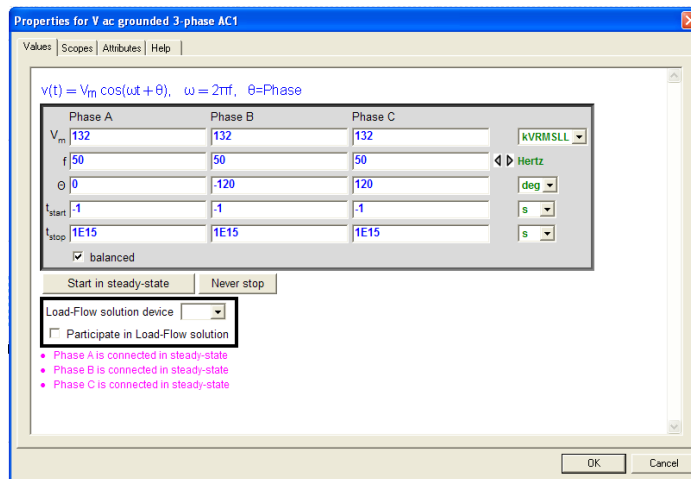


Figure 3.6(a): Circuit 1 AC source window

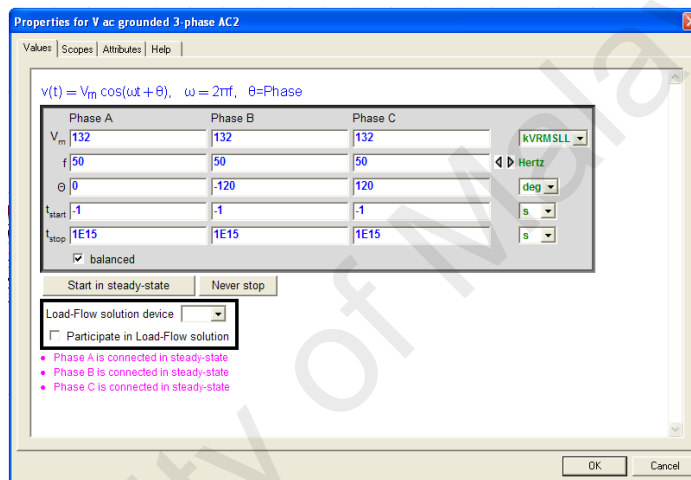


Figure 3.6(b): Circuit 2 AC source window

Figure 3.6: AC voltage source window

3.2.6 Lightning Strike and Striking Distance

The lightning wave shape was modelled based on CIGRE model, as shown in Figure 2.6 (CIGRE WG 33-01, 1991). Lightning stroke is represented as a current source with different magnitudes up to 200 kA. The peak current magnitude and tail time are important when observing the energy stresses of a surge arrester. The current wave front is an important parameter with regards to the insulator flashover. In this work, the front time and tail time used for normal operation is $2\mu\text{s}$ and $70\mu\text{s}$ respectively. The waveform is represented by the current front equation (3.5) and the current tail equation

(3.8) as follows:

$$I = At + Bt^n \quad (3.5)$$

where,

$$A = [1/(n-1)][(0.9I \times n/t_n) - S_m] \quad (3.6)$$

$$B = [1/t_n(n-1)][(S_m \times t_n) - 0.9I] \quad (3.7)$$

- t – instantaneous time
- t_n – front time passing through the 90% values of the current
- n – constant
- S_m – maximum front steepness

$$I = I_1 e^{-(t-t_n)/t_1} - I_2 e^{-(t-t_n)/t_2} \quad (3.8)$$

where,

- $I(t)$ – instantaneous lightning current
- I_1, I_2 – constant
- t_1, t_2 – times constant
- t – instantaneous time

Figure 3.7 shows the lightning current model used in the simulation. The lightning-path impedance, R_2 was represented by a resistance in parallel with a current source, which value was taken to be 400 Ω . Since the height of the transmission tower is less than 100 m, negative downward flash was chosen (Hileman, 1999).

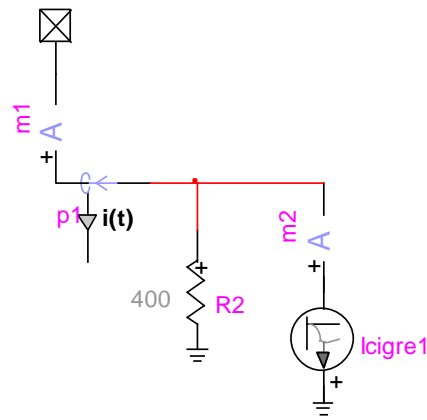


Figure 3.7: Lightning current model

3.2.6.1 Striking Distance

For effective shielding, it is better to determine the maximum lightning current, I_m that can be shielded by the ground wire, which no stroke will be terminated on the phase conductor. If lightning current is higher than I_m , it will be terminated on the ground wire or nearby ground. If the lightning current is lower than I_m , it will be terminated on the phase conductor. The striking distance to phase conductor, r_c and the striking distance to ground wire, r_g can be expressed by equation (3.9), where I is the lightning current (kA), and A and b are constant from Table 2.3. Constants from Brown and Whitehead (Brown & Whitehead, 1969) were chosen since they are suitable for vertical transmission line (Hileman, 1999).

$$r_c = r_g = AI^b \quad (3.9)$$

$$I_m = [r_{gm}/A]^{1/b} \quad (3.10)$$

$$r_{gm} = \frac{(h+y)/2}{1-\gamma \sin \alpha} \quad (3.11)$$

where

- h – ground wire height, m
- y – phase conductor height, m
- α – shielding angle, degree
- γ – r_g/r_c

The area that can be shielded by the ground wire is shown in Figure 3.8. Referring to equation (3.10), the maximum lightning current, I_m that can be shielded by the ground wire is 6.4 kA. According to the Lightning Detection System (LDS) in Malaysia, majority of the lightning current recorded on the 132kV KKRI-GMSG transmission line is higher than 80 Ka as shown in the Appendix A (Bakar, Othman, & Osman, 2007). Hence, shielding failure phenomena can be neglected in study.

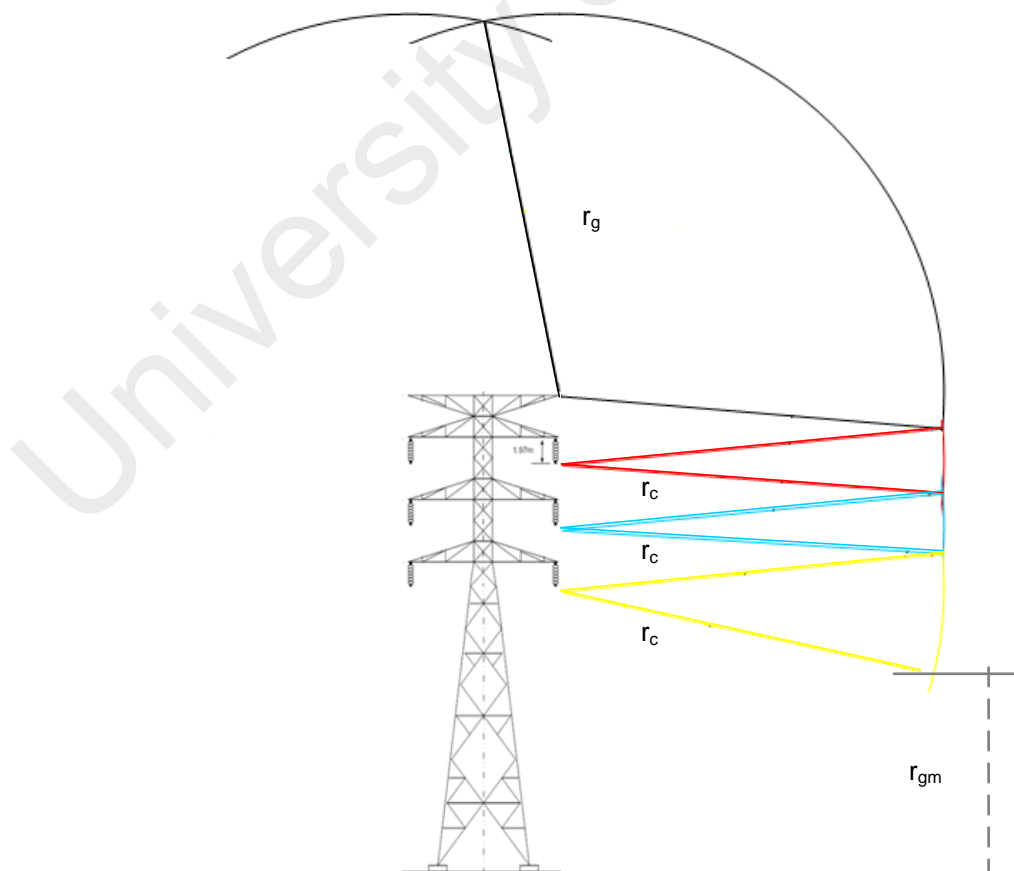


Figure 3.8 Conceptual diagram of lightning stroke to transmission line based on EGM

3.2.7 Surge Arrester

Surge arrester was designed based on the frequency dependent model recommended by IEEE WG 3.4.11, as depicted in Figure 3.9 (IEEE Std C62.22, 2009; IEEE Working Group 3.4.11, 1992). The two non-linear resistors separated by R-L filter are used to determine the non-linear V-I characteristics of the arrester. The R-L filter impedance is extremely low and A0 and A1 elements are connected in parallel during slow front surges. However, the filter impedance increases during fast front surges, resulting in a current distribution between the two non-linear resistances. Surge current with shorter front time will induce higher residual voltage since A0 resistance is practically greater than A1 resistance. The initial values for lumped parameter elements, L_0 , R_0 , L_1 , R_1 and C were determined using

$$L_1 = \frac{15d}{n} = 22.275 \mu H \quad (3.12)$$

$$R_1 = \frac{65d}{n} = 96.525 \Omega \quad (3.13)$$

$$L_0 = \frac{0.2d}{n} = 0.297 \mu H \quad (3.14)$$

$$R_0 = \frac{100d}{n} = 148.5 \Omega \quad (3.15)$$

$$C = \frac{100n}{d} = 67.34 pF \quad (3.16)$$

where

d – length of the arrester column in meters,

n – number of parallel columns of metal oxide disks in the arrester.

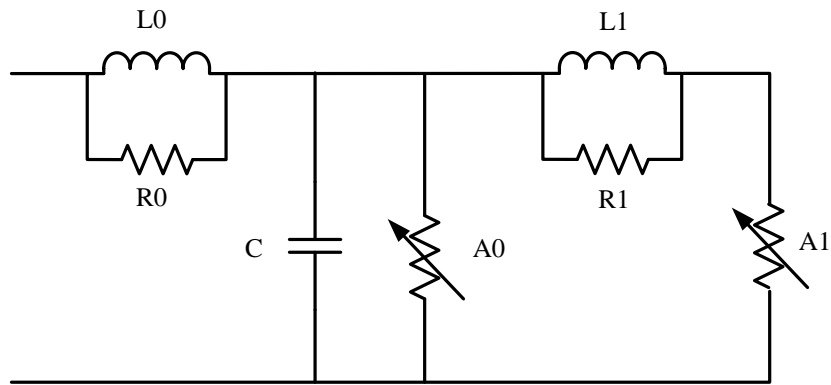


Figure 3.9 IEEE surge arrester circuit model

Table 3.3: describes the electrical and insulation characteristics of the designed surge arrester.

Table 3.3: Surge arrester characteristics

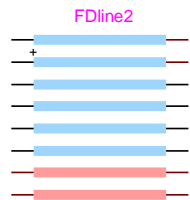
MCOV (Maximum Continuous Operating Voltage)	98 kV
Rated voltage	120 kV
Maximum residual voltage (lightning 8/20μs)	5kA 294 kV
	10kA 311 kV
	20kA 349 kV
Insulation material	Silicon rubber
Energy withstand	5.1 kJ/kV

3.2 Lightning Attachment

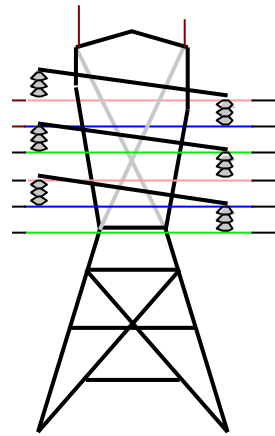
The model of double circuit transmission line in EMTP was tested by applying the lightning strikes at the ground wire on top of the tower. Figure 3.10 shows the complete test system of the 132 kV lines. Figures 3.10(a) to (d) show the model of the

transmission tower, transmission line, lightning and AC source voltage respectively. A 30 km line span was used to terminate both line ends to avoid any reflected travelling wave, which may affect the simulation of lightning overvoltage around the point of impact.

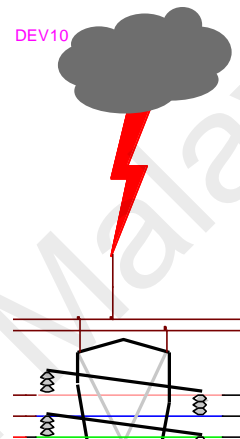
A single lightning stroke current was injected on the fifth tower top to create a flashover event across the line insulation. The lightning current was tested in the range of 30 kA to 225 kA and the footing resistance in the range of 10 Ω to 70 Ω as per actual site results, according to the 132 kV KKRI-GMSG tripping incidents occurring in year 2005. The tripping pattern due to the lightning back flashovers is determined by monitoring the voltage drop across the insulator string at each phase conductor on both circuits. Figure 3.10(e) shows the overall test system model.



(a) Transmission tower model

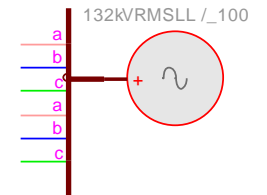


(b) Transmission line model

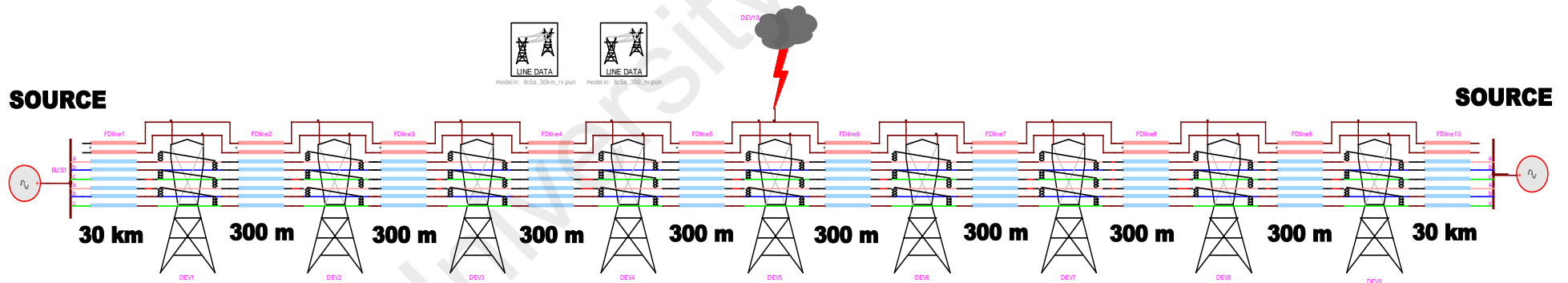


(c) Lightning attachment

SOURCE



(d) AC source voltage



(e) 132 kV test system model

Figure 3.10: 132 kV test system with lightning attachment model

3.3 Surge Arrester Placement

The tripping pattern behaviour of the test system helps to study the placement of the surge arrester for protection purpose. The arrester is connected between phase conductors and tower as shown in Figure 3.11. In this work, 6 different types of arrester configurations were studied to observe the arrester discharge energy. All configurations were tested by varying the lightning current, tower footing resistance, the point on wave of AC source voltage, number of tower, tail time, front time and span length to determine the most suitable arrester configuration.

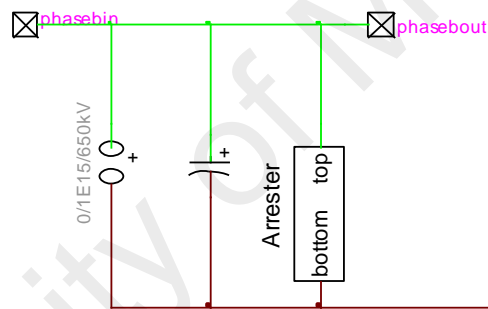


Figure 3.11: Surge arrester connection

CHAPTER 4

RESULTS AND DISCUSSION

4.1 Introduction

In this chapter, complete analysis and discussion on tripping pattern and surge arrester discharge energy obtained from the simulated results are presented. The analysis is based on back flashover studies conducted to observe discharge energy during lightning strike termination on ground wire. This chapter also aims to investigate competency of the installed arrester in providing the best lightning protection for transmission line system in term of maximum energy absorption as well as complying with the TNB's design requirement.

Simulation results obtained from EMTP-RV for flashover tripping is recoded when the phase conductor's voltage drop to zero. Figure 4.1 shows waveforms of the voltage drop at insulator string for red phase of double circuit transmission line after being strike by lightning at the ground wire of the study tower. The voltage drop for each phase conductors is not the same. The line is considered trip when the insulator voltage of phase line drops to zero as shown in Figure 4.1 (b).

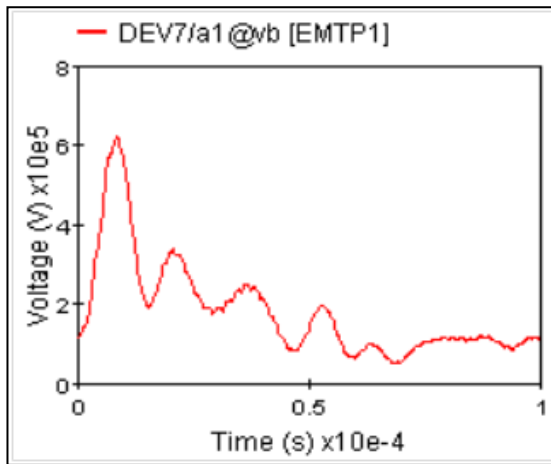


Figure 4.1(a): Red phase voltage for Circuit 1

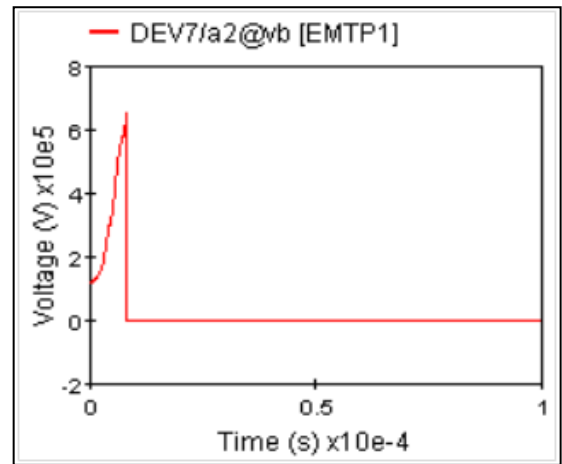


Figure 4.1(b): Red phase voltage for Circuit 2

Figure 4.1: Voltage drop at Double Circuit Line

The second part of this study is to determine the total energy absorption of the designed arrester due to lightning terminating on a ground wire. The value of energy is recorded when it is constant at certain value as shown in Figure 4.2. The tripping patterns and surge arrester discharge energy may vary depending on the magnitude of lightning current, the point on wave of AC source, the arrangement of phase conductors on the tower or the value of tower footing resistance during the lightning strike. These factors are discussed in more details in the next section.

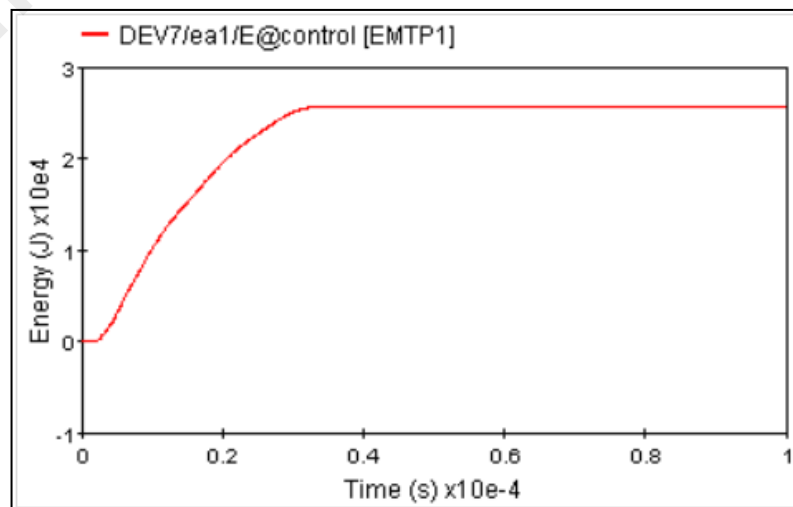


Figure 4.2: Discharge energy of surge arrester

4.2 Analysis of Tripping Pattern without Surge Arresters

The following section presents the back flashover tripping patterns for the 132 kV double circuit transmission line, which were obtained based on the previous study (Bakar et al., 2013). Any phase where flashover occurs during a stroke at tower top is denoted by 'X', as summarized in Tables 4.1 to 4.3. The influence of lightning current magnitude, tower footing resistance and point on wave of AC source voltage on the line lightning performance were also considered to further analyse the optimised surge arrester (SA) configuration required for eliminating double circuit outages due to back flashover.

4.2.1 Lightning Current Magnitude

The impact of lightning current magnitude on the insulator flashover is presented in Table 4.1. Five different magnitudes ranging from 110 kA to 200 kA were injected to the tower top, while the voltage reference angle and tower footing resistance were maintained at 100° as shown in Figure 4.3 and 10Ω .

Table 4.1: Insulator flashovers for different lightning current magnitudes

Lightning current (kA)	Flashover (X)					
	Circuit 1			Circuit 2		
	R	B	Y	R	B	Y
110					X	
122		X			X	
150		X		X	X	
175	X	X	X	X	X	
200	X	X	X	X	X	X

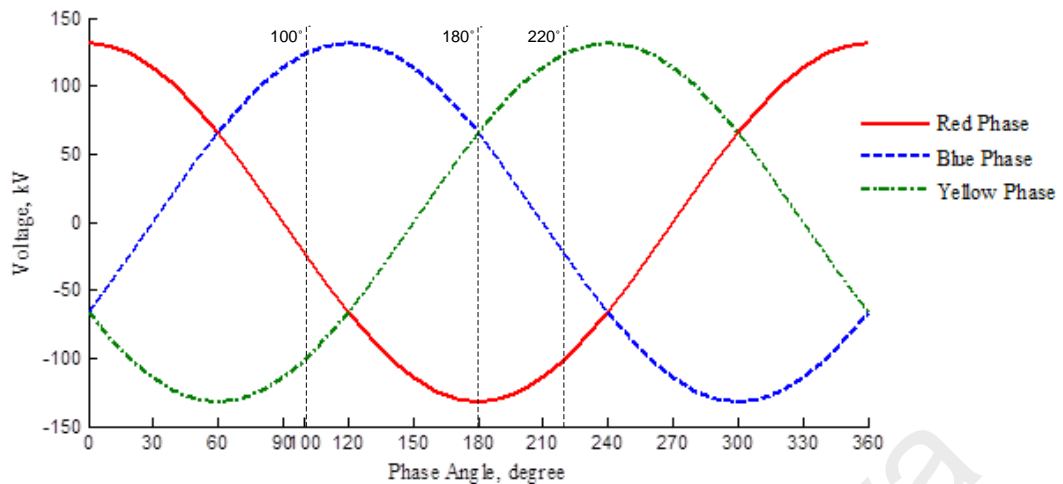


Figure 4.3 Power frequency voltage as a function of phase angle 100°, 180° and 220°

It is observed that a lightning current magnitude of 110 kA causes single circuit flashover across blue phase insulation at circuit 2. Increasing the magnitude of the lightning stroke from 122 kA to 200 kA results in higher probability of a double circuit outage. Hence, the results indicate that the back flashover tripping pattern is influenced by the lightning current magnitude. Further validation has also proven that the overall simulated results were in good agreement with the previously published data (Bakar, et al., 2013).

4.2.2 Tower Footing Resistance

The tower footing resistance was varied from 5 Ω to 50 Ω to determine its dependency on the flashover tripping pattern. Table 4.2 represents the insulator flashovers when the lightning current magnitude and voltage reference angle were simulated at 122 kA and 100°. Lightning current magnitude of 122 kA was chosen because at this particular value, double circuit tripping occurs as depicted in Table 4.1. Therefore, there is

unimportant to choose magnitude below 122 kA as this work focuses on mitigating double circuit outages.

Table 4.2: Insulator flashovers for different tower footing resistances

Footing resistance (Ω)	Flashover (X)					
	Circuit 1			Circuit 2		
	R	B	Y	R	B	Y
5						
10		X			X	
20	X	X		X	X	
30	X	X	X	X	X	X
50	X	X	X	X	X	X

In case of a lightning strike to tower top, the overvoltages developed across the insulator strings strongly depend on the footing resistance value of the struck tower and the adjacent towers. Flashover occurs at both circuits of the struck tower when the footing resistance is more than 10 Ω . The results also indicate that the resistance value of 30 Ω and higher causes flashover of all three phases of the struck tower. Therefore, maintaining a low tower footing resistance is essential to prevent a double circuit outage, which partially improves lightning protection of the transmission line.

4.2.3 Point on Wave of AC Source Voltage

In order to investigate the influence of power frequency voltage on the flashover performance, a lightning current of 200 kA was injected at the tower top by keeping the tower footing resistance constant at 10 Ω . From Table 4.3, the tripping patterns of phase conductor differ with varying phase voltage angle due to different voltage magnitude.

According to Table 4.3, both blue and yellow phases experience double circuit outages when the voltage reference angle was simulated at 180° and 220°. At that particular angle, Figure 4.3, the voltages of blue and yellow phases are much higher compared to red phase voltage, causing both phase insulation to be more probable to flashover (Bakar et al., 2013). Hence, the instantaneous power frequency voltage has a significant contribution on the overvoltage induced due to back flashover.

Table 4.3: Insulator flashovers for different phase voltage angles

Phase angle (deg°)	Flashover (X)					
	Circuit 1			Circuit 2		
	R	B	Y	R	B	Y
0	X	X	X	X	X	
70	X	X	X	X	X	
120	X	X	X	X	X	X
180		X	X		X	X
220		X	X		X	X
300	X		X	X	X	X

4.3 Analysis of Tripping Pattern with Surge Arresters

The effectiveness of surge arrester (SA) configurations to improve the line flashover performance is discussed in the following section. Any simulated case without flashover occurrence is denoted as 'ŃT'. 'ŠT1' and 'ŠT2' denotes a single circuit tripping for circuit 1 and circuit 2 respectively due to back flashover while a double circuit tripping is denoted by 'ĐT', as summarized in Table 4.4 to Table 4.6. The best possible configuration is determined based on the capability to mitigate double circuit tripping.

4.3.1 Lightning Current Magnitude

The effects of SA configurations with respect to lightning current magnitude on the flashover performance are demonstrated in Table 4.4. Five different magnitudes ranging from 122 kA to 225 kA were injected to the tower top, while the voltage reference angle and tower footing resistance were maintained at 100° and 10 Ω. Configuration 7 shows the tripping pattern for tower without surge arrester. In case of lightning strokes higher than 122 kA, installation of SAs is crucial to prevent double circuit tripping due to back flashover. The results indicate that configuration 1 is able to eliminate insulator flashovers on both circuit for current magnitudes up to 200 kA. However, configuration 1 does not improve the line lightning performance where it is only able to mitigate the double circuit tripping for a current magnitudes less than 200 kA.

Table 4.4: Insulator flashover patterns for different lightning current magnitudes

No.	SA Configuration	Lightning Current, I_{peak} (kA)				
		122	150	175	200	225
1		ŇT	ŠT2	ŠT2	ŠT2	ĎT
2		ŇT	ĎT	ĎT	ĎT	ĎT
3		ŇT	ŠT2	ŠT2	ŠT2	ŠT2
4		ŇT	ŠT2	ŠT2	ĎT	ĎT
5		ŇT	ŠT2	ŠT2	ŠT2	ŠT2
6		ŇT	ŇT	ŇT	ŇT	ŇT
7		ĎT	ĎT	ĎT	ĎT	ĎT

●SA ŇT-No Tripping ŠT2-Single circuit 2 tripping ĎT-Double circuit tripping

The presence of SAs on the lower phase of the first circuit and the upper phase of the second circuit as per configuration 2 results in the worst lightning protection, at which double circuit outages tend to occur for lightning strokes higher than 150 kA.

Configurations 3 and 4 demonstrate the same flashover characteristics for lightning current magnitudes up to 175 kA. However, configuration 4 is unable to protect the line against double circuit flashover for magnitudes of above 200 kA. The flashover performance of configuration 5 is much better compared to configuration 4 even though the same numbers of SAs were installed on all phases regardless of positioning on the circuit. The installed SAs effectively perform the discharge duty without experiencing any double circuit flashover up to 225 kA.

Based on the simulated results, simultaneous double circuit line outages due to variation in the lightning current magnitudes striking the tower top could be significantly eliminated by incorporating configuration 3 or 5 in the designed system. For a relatively low tower footing resistance up to 10Ω , is it sufficient enough to consider installation of three SAs at the struck tower. However, configuration 6 has an advantage over configurations 3 and 5, where the probability of insulator flashover is reduced to zero by installing the SAs on all three phases of both circuits. The configuration could be incorporated for cases with high tower footing resistance since the three SAs positioned in one circuit will not be able to prevent double circuit outages occurrence due to back flashover on adjacent towers.

4.3.2 Tower Footing Resistance

The improvement in flashover performance of the line for different tower footing resistances is depicted in Table 4.5. The lightning current magnitude and voltage reference angle were simulated at 122 kA and 100° . Configuration 7 shows the tripping results for transmission line without SA. As discussed from previous section, the tower that has footing resistance higher than 10Ω will experience double circuit tripping.

Table 4.5: Insulator flashover patterns for different tower footing resistances

No.	SA Configuration	Footing Resistance, R_f (Ω)					
		5	10	20	30	50	70
1		ŇT	ŇT	ĎT	ĎT	ĎT	ĎT
2		ŇT	ŇT	ĎT	ĎT	ĎT	ĎT
3		ŇT	ŇT	ŠT2	ĎT	ĎT	ĎT
4		ŇT	ŇT	ĎT	ĎT	ĎT	ĎT
5		ŇT	ŇT	ŠT2	ŠT2	ŠT2	ŠT2
6		ŇT	ŇT	ŇT	ŇT	ŇT	ŇT
7		ŇT	ĎT	ĎT	ĎT	ĎT	ĎT
●SA		ŇT–No Tripping		ŠT2–Single circuit 2 tripping		ĎT–Double circuit tripping	

For footing resistance values of 5 Ω and 10 Ω , no insulator flashover was observed for Configurations 1 to 6. This provides justification on the importance of maintaining a low footing resistance value as one of the mitigation measures to prevent flashovers. Furthermore, Configurations 1 and 2 result in double circuit outages for resistance value of 20 Ω and above. It is also observed that Configuration 3 provides a better lightning protection as compared to Configuration 4, where it is capable of eliminating double circuit tripping when the resistance was simulated at 20 Ω . Hence, Configurations 1, 2 and 4 do not offer sufficient protection to prevent a double circuit flashover occurrence for resistance greater than 10 Ω .

Installation of SAs on all phases of one circuit as depicted by Configuration 5 successfully inhibits the simultaneous line outages, where the continuity of service of one circuit was sustained for a very high value of resistance up to 70 Ω . Configuration 6 completely improves the flashover performance of the 132 kV line, where zero circuit tripping was drawn for all resistance values. However, installation of SAs on all phases of both circuits is unnecessary unless the design objective is to completely eliminate the

flashovers. Although an optimum lightning protection may be achieved, the configuration does not provide an economical solution as excessive number of installed SAs will only lead to failure caused by high energy stress.

4.3.3 Point on Wave of AC Source Voltage

Optimum configuration was also determined based on the flashover performance with respect to the instantaneous power frequency voltage, as demonstrated in Table 4.6. The ability of each configuration to restrain insulator from experiencing flashover was investigated by simulating a very high lightning stroke magnitude of 200 kA at the tower top.

Table 4.6: Insulator flashover pattern for different power frequency angles

No.	SA Configuration	Power frequency angle (deg°)					
		0	70	120	180	220	300
1		ĐT	ĐT	ĐT	ĐT	ĐT	ĐT
2		ĐT	ĐT	ĐT	ĐT	ĐT	ĐT
3		ĐT	ŠT2	ŠT2	ĐT	ĐT	DT
4		ĐT	ĐT	ŠT2	ŠT2	ŠT2	ĐT
5		ŠT2	ŠT2	ŠT2	ŠT2	ŠT2	ŠT2
6		ŃT	ŃT	ŃT	ŃT	ŃT	ŃT
7		ĐT	ĐT	ĐT	ĐT	ĐT	ĐT

●SA ŃT–No Tripping ŠT2–Single circuit 2 tripping ĐT–Double circuit tripping

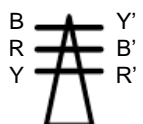
Configuration 6 demonstrates the same lightning performance derived from the previous sections, where no line tripping was initiated from back flashover phenomenon. Incorporating two SAs at the struck tower does not provide a complete protection against double circuit line flashover for each phase angle step, as depicted by

Configurations 1 and 2. As for Configurations 3 and 4 which have the same number of SAs installed, inconsistent tripping pattern shows by varying the voltage point on wave. Configuration 5 notably improves the lightning performance where the presence of SAs on all phases of single circuit prevents the overvoltage from inducing double circuit flashover.

4.4 Analysis of Surge Arrester Discharge Energy Capability

The effectiveness of surge arrester (SA) configurations by considering the discharge energy to improve the line flashover performance is discussed in this section. There are 6 types of SA configurations suggested in this work as shown in Table 4.7. Analyses were done by comparing the discharge energy of all configurations during a lightning stroke to the tower top. The best configuration is determined from its ability to protect the transmission line from double circuit tripping and complying with the required energy discharge capability of 5.1 kJ/kV of MCOV. Note that for all simulated cases, the highest measured energy of one SA among the installed SAs at the struck tower was determined for each configuration to estimate the energy discharge capability.

Table 4.7: Surge arrester configurations

SA Configuration	1	2	3	4	5	6
						

4.4.1 Lightning Current Magnitude

The lightning current magnitude was varied to investigate its influence on the discharge energy. The tower footing resistance and voltage reference angle were fixed at $10\ \Omega$ and 100° respectively. A nonlinear increment is observed on the SA discharged energy with the increase of the peak lightning current magnitude, as illustrated in Figure 4.4. The lowest energy for each configuration was measured at stroke magnitude of 122 kA while the highest energy was measured at 225 kA. This phenomenon arises when higher stroke magnitude causes more discharge current to flow across the arrester, producing higher energy level stressed on it. Furthermore, the results indicate that the discharged energy for Configurations 3, 4 and 5 slightly differ from each other since a similar number of SAs were installed at the struck tower, which is three. However, a significant difference in the discharge energy is observed for Configurations 1 and 2 even though they were constructed with two SAs.

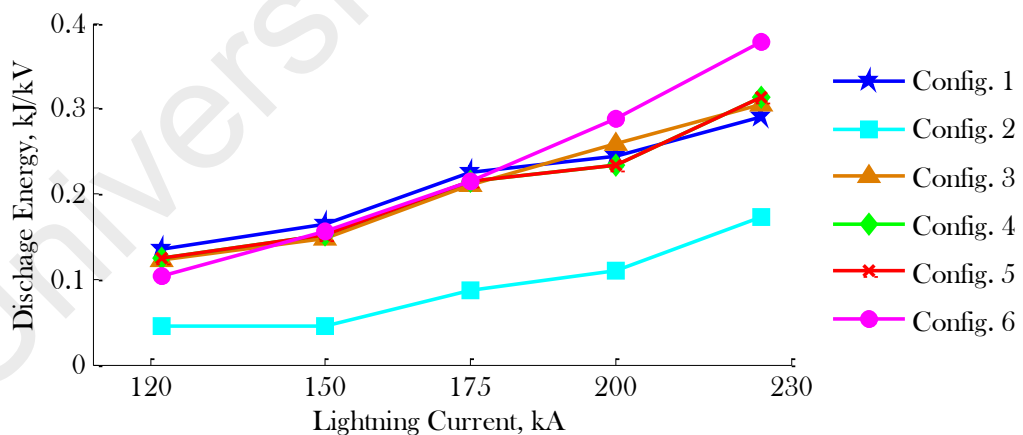


Figure 4.4: SA discharge energy as a function of lightning current magnitude

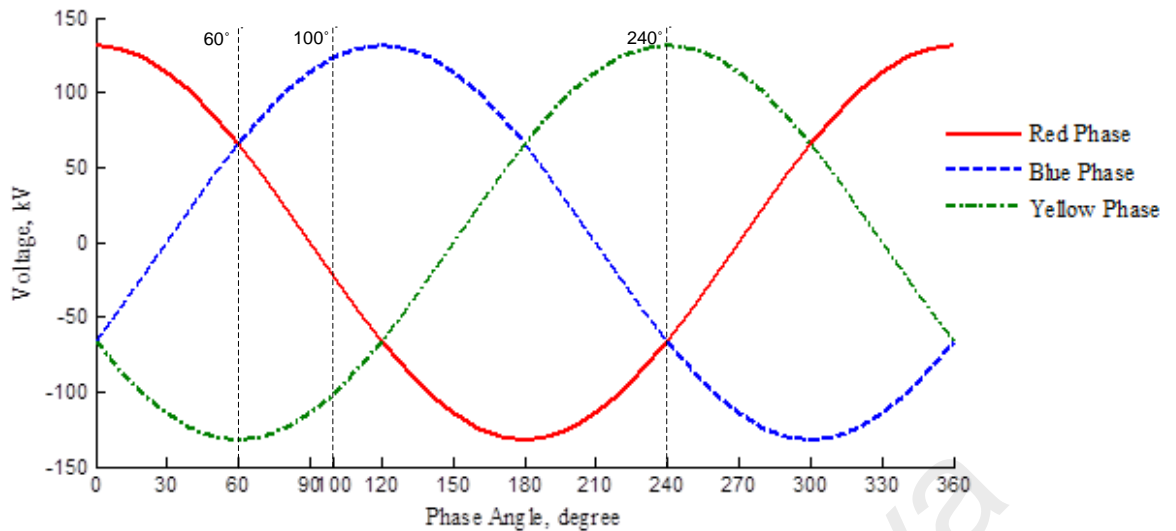


Figure 4.5: Power frequency voltage as a function of phase angle 60°, 100° and 240°

Configuration 2 produces lower amount of energy than Configuration 1 since there is no SA installed at blue phase of Configuration 2. This is due to the effect of power frequency voltage on the induced voltage across the phase insulation. Referring to Figure 4.5, blue phase has the maximum power frequency voltage at the reference angle of 100°. During back flashover event, the SA installed at blue phase of Configuration 1 will experience high energy discharge duty, as higher voltage resulting from the power frequency voltage and lightning overvoltage is developed across the insulation.

4.4.2 Tower footing resistance

A constant representation of tower footing resistance was considered in this study to analyse its effect on the SA discharge energy. For each configuration, the resistance value was varied from 5 Ω to 70 Ω while the voltage reference angle and lightning current magnitude were maintained at 100° and 122 kA respectively. As illustrated in Figure 4.6, the SA discharged energy increases with respect to the tower footing resistance.

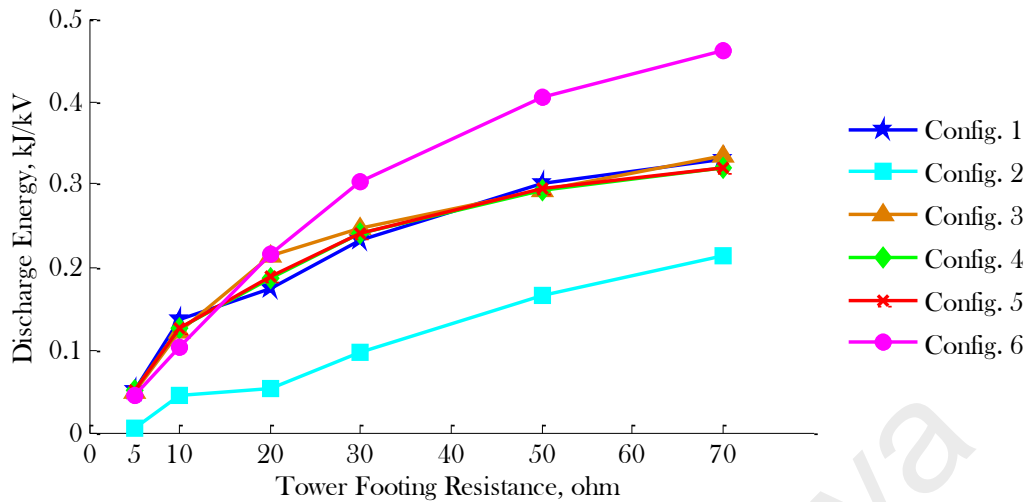


Figure 4.6: SA discharge energy as a function of tower footing resistance

A significant increment in the energy level is observed for the resistance value of more than 20 Ω . High resistance causes larger stroke current to be discharged through the installed SAs, which will then result in greater energy level. Hence, maintaining a low tower footing resistance is essential so that more stroke current will be diverted to ground. This helps to decrease the lightning overvoltage built across the insulator string as more negative reflections are produced from the tower base towards the tower top, reducing the probability of SA failure due to high energy discharge duty. The findings also clearly indicate that the installed SAs for each configuration were capable of surviving the energy dissipated from the lightning stroke current and conforming to the standard design requirement.

4.4.3 Point on Wave of AC Source Voltage

The effect of power frequency voltage on the maximum discharge energy was determined by varying the voltage reference angle (red phase) in the range of 0° to 300° , as shown in Figure 4.7.

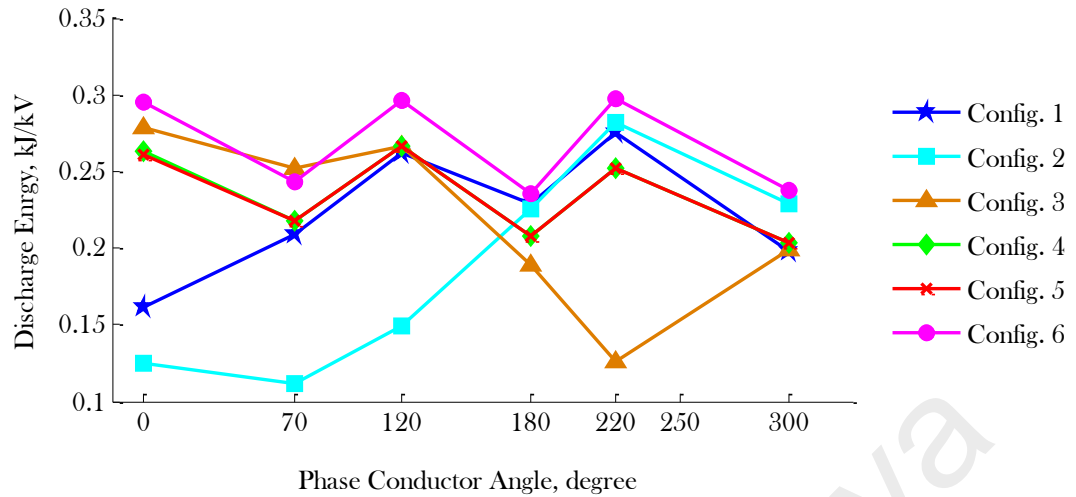


Figure 4.7: SA discharge energy as a function of phase conductor angle

Constant lightning current magnitude of 200 kA (2/70 μ s) and footing resistance of 10 Ω were selected for all simulated cases. It can be deduced that the energy discharged vary for different value of voltage reference angle. This phenomenon can be further explained by referring to Figure 4.5. During normal operating condition, the maximum voltage across the insulation is observed at alternate times on red, blue and yellow phases. When lightning overvoltage occurs, the maximum voltage developed across the phase insulation is dependent on the magnitude of the instantaneous power frequency voltage and the incoming surge. Thus, the phase angle at the instant of lightning stroke termination influences the insulator flashover, where the probability of flashover to occur is higher at the phase conductor with higher power frequency voltage. As more voltage is built up across the insulation, the installed SAs will experience higher energy discharged duty to protect the phase conductor from flashover occurrence.

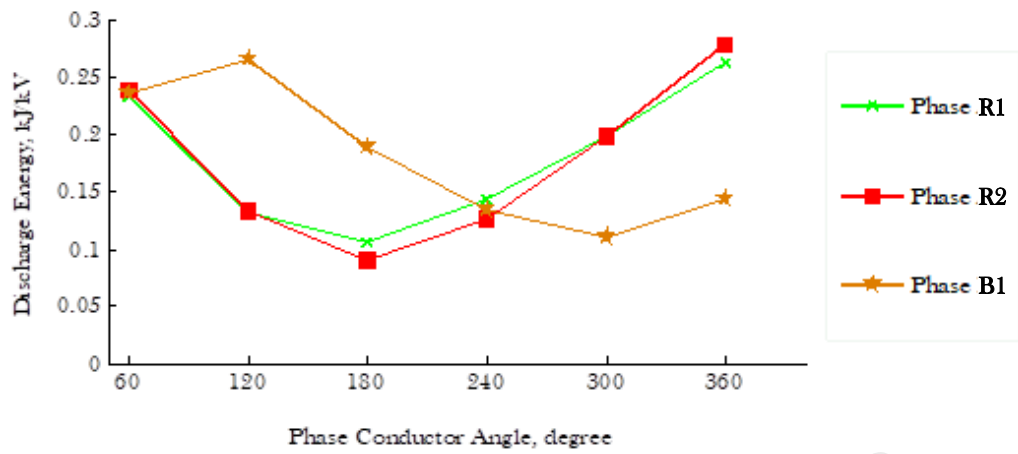


Figure 4.8(a): Configuration 3

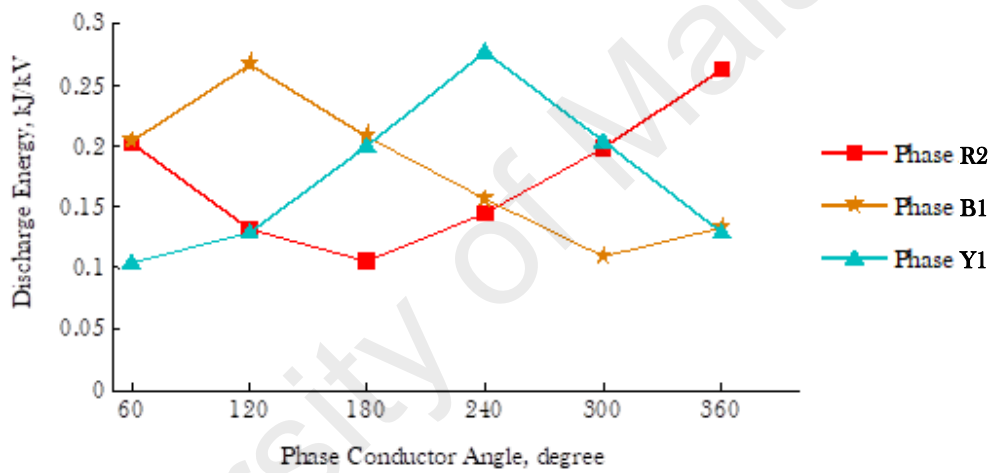


Figure 4.8(b): Configuration 4

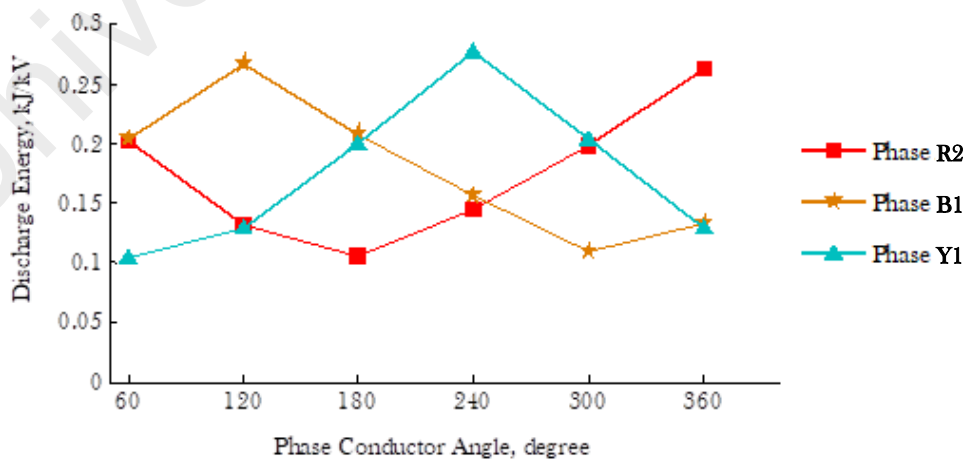


Figure 4.8(c): Configuration 5

Figure 4.8 Discharge energy of SA at different phases as a function of phase conductor angle

A comparison was made on the energy stress obtained from Configurations 3, 4 and 5 to further investigate the influence of the power frequency effect, as depicted in Figure 4.8. The results demonstrate that the SAs at red and blue phases absorbed approximately the same amount of energy when the angle was simulated at 60° and 240°. This is due to intersection of both phases at the same angle, causing the same amount of voltages observed across the phases insulations, as shown in Figure 4.5. Furthermore, at the angle of 240° the maximum energy was discharged by SA installed at yellow phase since the phase voltage is higher than the other phases. Based on the previous discussion, more energy will be dissipated through the SA when higher voltage is built up due to surge voltage and phase voltage. Hence, this phenomenon successfully validates that the power frequency voltage has a great influence on the SA discharge energy.

4.4.4 Effect of number of towers

The effect of installing SAs on the maximum discharge energy is studied by considering 6 configurations of SAs and 5 different numbers of towers as shown in Table 4.8. The voltage reference angle, footing resistance and lightning current magnitude were maintained at 100°, 10 Ω and 200 kA respectively. The maximum discharge energy from one of the SA (for each of the SA configuration) at the stuck tower and its corresponding number of tower is shown in Table 4.8.

Table 4.8: SA discharged energy (kJ/kV) as a function of number of tower

No.	SA Configuration	Number of tower				
		3	5	7	9	13
1		0.156	0.199	0.225	0.244	0.256
2		0.086	0.098	0.109	0.109	0.119
3		0.157	0.201	0.236	0.259	0.279
4		0.148	0.189	0.217	0.234	0.248
5		0.148	0.189	0.217	0.234	0.248
6		0.161	0.237	0.269	0.288	0.302

●Surge arrester

For each configuration, the results indicate that the energy increases with respect to the number of towers included in the model. This phenomenon is initiated when the discharged current flows through the adjacent SAs are of reverse direction to the discharged current through the struck SAs. The opposite polarity current will then travel back to the lightning stroke termination point, resulting in higher energy levels of the struck SAs. It should be noted that the surge arrester does not absorb all of the high voltage that passes through it. It simply diverts it to the ground or clamps it to minimize the voltage that passes through it. On the other hand, it is evident that a constant amount of energy was discharged when the numbers of towers simulated in the model are not less than seven. A significant deviation is observed in the discharged energy for lower number of towers. Incorporating a higher number of towers installed with SAs will also reduce the probability of insulators to flashover by obviating the surge waveform from travelling further. Hence, these justify the importance of selecting the appropriate number of towers to be included in the designed system to accurately calculate the energy stress.

4.4.5 Effect of span length

The effect of varying span length on the maximum SA discharged energy at the struck tower is shown in Figure 4.9. Lightning current magnitude and voltage reference angle were kept constant at 200 kA (2/70 μ s) and 100° respectively.

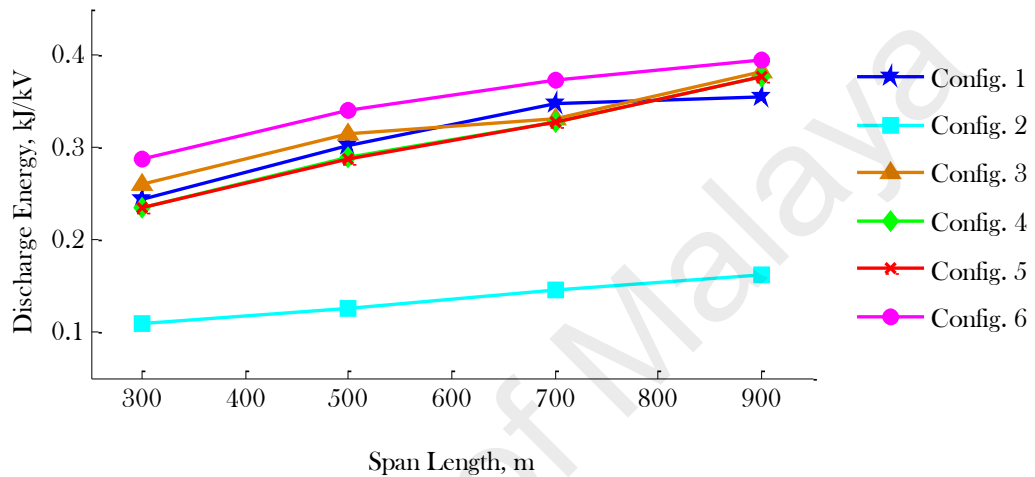


Figure 4.9: SA discharged energy as a function of span length

Increasing the line span length will result in higher energy absorbed by the arrester. A lightning stroke to the tower top causes the current to split into one flowing left and right through the ground wire and one flowing through the tower (Hileman, 1999; Pham et al., 2012).

If the line span is longer, a greater value of line inductance will be produced (4.1), causing the line impedance to increase (4.2). This will result in more lightning current flow to the tower, rather than through the ground/shield wires. The tower voltage will be higher, causing more current flow through the arresters and therefore energy absorbed by the arresters are higher.

$$Z_g = \sqrt{L/C} \quad (4.1)$$

$$L = (Z_g/v) \times \text{span length} = Z_g T_s \quad (4.2)$$

$$T_s = \text{spanlength}/v \quad (4.3)$$

$$\tau = (Z_g/R_i) \times T_s \quad (4.4)$$

$$W_A = i_A E_A \tau \quad (4.5)$$

where,

Z_g – ground wire impedance, Ω

L – line inductance, μH

C – line capacitance, μF

T_s – travelling time of the line span, μs

v – speed of light, $\text{m}/\mu\text{s}$

τ – time constant, μs

R_i – tower footing resistance, Ω

W_A – SA discharge energy, kJ

i_A – SA discharge current, kA

E_A – SA discharge voltage, kV

The dependency of arrester discharge energy on the transmission line span length can also be validated by equations (4.2) to (4.5). From (4.2), it can be observed that the line inductance relies on the ground wire impedance (Z_g) and travelling time (T_s) of the line span. Hence, by simulating a longer line span, T_s will increase and a greater value of the line inductance (L) will be produced. Consequently, the time constant (τ) which is highly dependent on the inductance value will also be increased, resulting in an increase in the energy discharged by the arrester (Hileman, 1999; McDermott, 2006).

A slight difference was observed on the measured discharge energy for Configurations 5 and 6. However, the discharged energy is greater for Configuration 3 than Configurations 4 and 5 even though the number of SAs installed for all cases are the same. This might be due to the effect of phase conductors positioning, where for Configuration 3, SAs were installed only on red and blue phases. Both circuits of yellow phase, which have the lowest coupling factor with ground wire, were not equipped with SA, thus, causing an increase in the energy discharged through the SAs.

Simulations were also performed to investigate the impact of lightning stroke termination point on the SA discharge energy. Table 4.9 presents the maximum energy when lightning struck directly on top of the middle tower and at the mid span between the fourth and fifth tower. Due to lower discharged energy across the adjacent SAs, a stroke to mid span results in only 17-30% energy stress of that for a stroke to the tower top. The effect of lightning stroke termination between towers can be neglected since a strike to tower top produces a more significant impact on the discharged energy.

Table 4.9: Discharged Energy for Stroke to Tower and Mid Span

No.	SA Configuration	Discharged energy (kJ/kV)		Difference (%)
		Tower	Mid span	
1		0.243605	0.072953	29.9
2		0.109406	0.018889	17.3
3		0.2595	0.065388	25.2
4		0.234356	0.066161	28.2
5		0.234361	0.066683	28.4
6		0.287794	0.056689	19.7

●Surge arrester

4.4.6 Effect of tail time

Varying the time to half, t_h , or tail time of the lightning wave shape significantly increases the maximum discharge energy. Figure 4.10 illustrates the results obtained for several t_h values, by keeping constant the voltage reference angle, footing resistance, lightning current magnitude and front time at 100° , 10Ω , 200 kA and $2\mu\text{s}$ respectively.

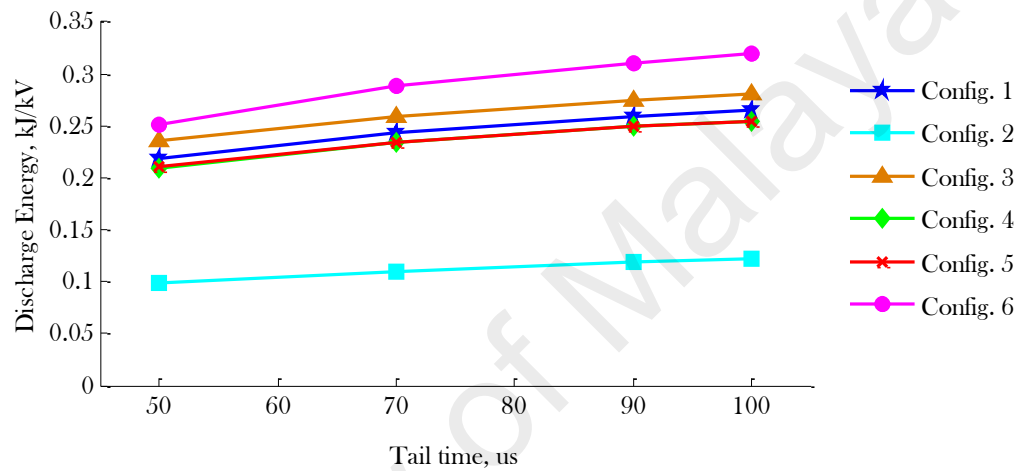


Figure 4.10: SA discharged energy as a function of tail time

The discharged energy is dependent on the duration of the lightning impulse current flowing through the SA. This happens as the accumulated instantaneous power stressing the SA influences the energy discharge duty, as validated by (Savic, 2005):

$$W_A = \int_{t_0}^t u_A i_A dt \quad (4.6)$$

where,

- W_A – SA discharge energy, J
- t – current time instant, s
- t_0 – time at which the lightning overvoltage appears at the SA terminal, s
- u_A – instantaneous SA discharge voltage, A
- i_A – instantaneous SA discharge current, A

For a fixed value of lightning peak current, the energy discharged increases with respect to the duration of tail time. For example, a current waveform of 70 μ s tail time decays slower to its half value as compared to a current waveform of 50 μ s tail time, as demonstrated in the Figures 4.11 (a) and (b). The phenomenon happens as a longer tail time increases the tail time constant (τ), which may cause the current waveform to extinguish slower. As the duration of lightning current stressing the arrester increases, the energy discharged will be greater. This provides justification on the importance of tail time effect when observing energy stress of surge arrester.

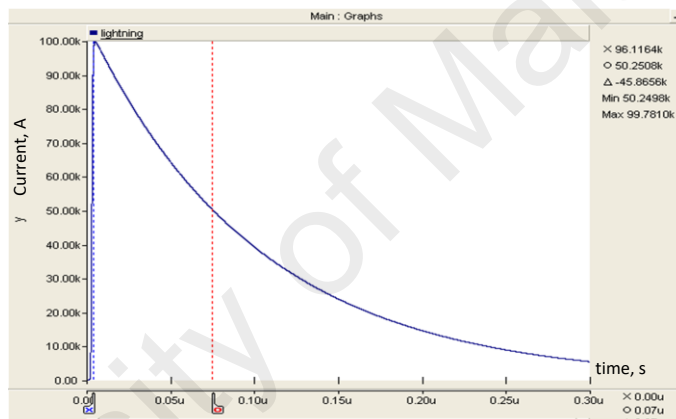


Figure 4.11(a): 2/70 μ s current waveform

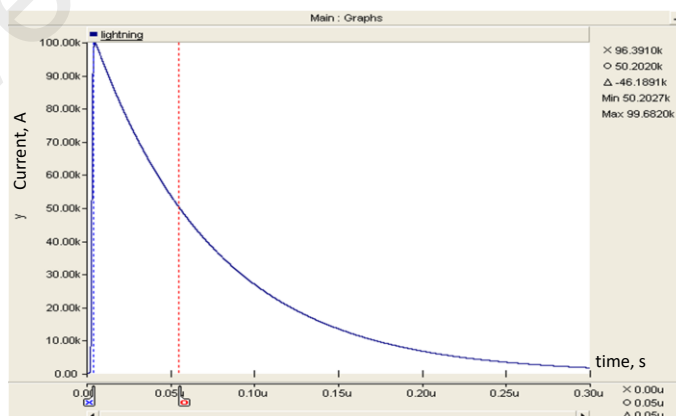


Figure 4.11(b): 2/50 μ s current waveform

Figure 4.11: Lightning current waveform for different tail time

4.4.7 Effect of front time

The effect of lightning stroke front time, t_f , was deduced by simulating different current wave shape. Figure 4.12 depicts the measured discharge energy when the front time was varied between $1.5\mu\text{s}$ and $2.5\mu\text{s}$. The voltage reference angle, footing resistance, lightning current magnitude and time to half were kept constant at 100° , $10\ \Omega$, $200\ \text{kA}$ and $70\ \mu\text{s}$ respectively. For each configuration, it is evident that the front time has a negligible influence on the discharge energy even though a high lightning current was chosen to demonstrate the effect. Therefore, the front time should not be a great concern in selecting lightning stroke parameters for SA energy determination.

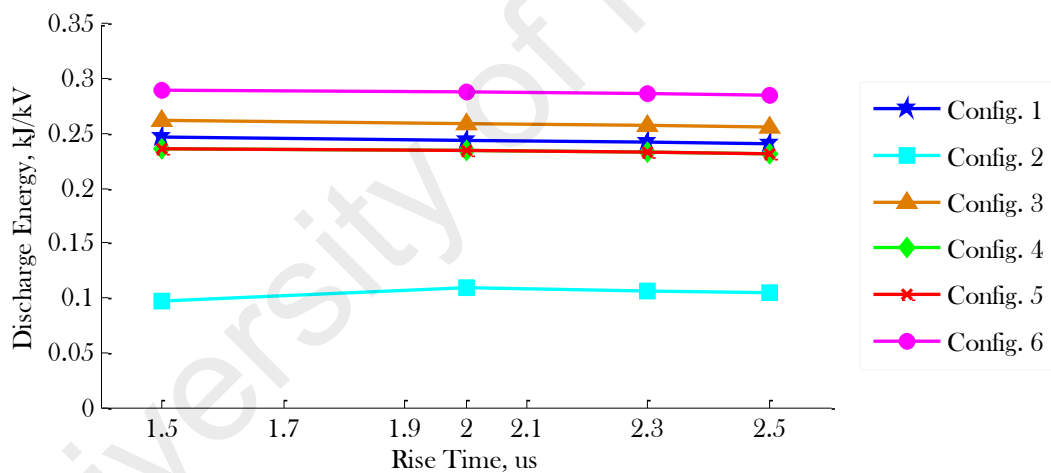


Figure 4.12: SA discharged energy as a function of rise time

4.5 Summary

A 132 kV double circuit overhead transmission line was modelled to investigate the capability of the designed transmission line surge arresters in withstanding the lightning energy during back flashover event and eliminating double circuit tripping. From the simulation, it was observed that higher lightning current and tower footing resistance results in higher probability of a double circuit tripping. The tripping patterns of phase conductor differ with various point on wave of AC source voltage due to different voltage magnitude. Hence, the instantaneous power frequency voltage has a significant contribution on the overvoltage induced due to back flashover. From simulation of various surge arrester installations on transmission lines, it shows that when surge arresters are installed on all phases of one of the circuits, double circuit tripping can be eliminated. Higher tower footing resistance, current magnitude, number of tower, span length and tail time causes the SAs to discharge higher energy.

CHAPTER 5

CONCLUSIONS AND RECOMMENDATIONS

5.1 Conclusions

The capability of surge arresters installed on a 132 kV double circuit transmission line in withstanding current and energy discharged by lightning strikes during back flashover phenomena has been successfully studied using Electromagnetic Transient Program (EMTP-RV). Installation of surge arresters (SA) with appropriate rating on all phases of a single circuit successfully reduces the possibility of simultaneous double circuit flashover due to a lightning stroke to the tower top. However, the configuration was unable to prevent the likelihood of single circuit outages on the unprotected parallel circuit. If the design objective mainly emphasizes on reducing the probability of insulator flashovers to zero, installing the SAs on one or more phases of the unprotected circuit should be a great concern. The configuration could be incorporated for the tower footing resistance value of more than 10 Ω since the configuration with three SAs equipped in one circuit was incapable in eliminating double circuit flashovers at very high lightning currents.

The degree of protection offered by each configuration was also measured based on their energy discharge duty. A significant increment in the maximum discharged energy was observed with the increase of lightning current, tower footing resistance, tail time and span length. The simulated maximum energy stresses for all configurations were below the rated discharged energy of 5.1 kJ/kV. An improved lightning performance could be achieved by increasing the number of phases on which SAs are installed since

the total energy absorption capability will be higher. However, installing the SAs on all phases of a double circuit transmission line is redundant for a relatively low tower footing resistance up to 10 Ω , as the configuration might lead to the risk of failure due to energy stress.

Installing surge arresters on all phases at one of the circuit provides a sufficient lightning protection level due to its ability to reduce the risk of a double circuit outage occurrence. This configuration also complies with the rated energy handling capability of 5.1 kJ / kV for MCOV, currently utilized by the national utility company for a 132 kV transmission line. Therefore, the best surge arrester configurations in 132 kV transmission line have been identified from this work.

5.2 Recommendations

This study could be further extended by improving the modelling approach to achieve better results and findings. The recommendations are:

- a) Multiple strokes lightning (MSL) can be used to simulate lightning overvoltage since most of the lightning strikes consist of more than a single stroke (SSL).
- b) Various modelling methods for lightning current source and fast front surge arrester can be carried out to develop future studies which are more practical to power system transient analysis.
- c) Study on the quadruple circuit transmission line, such as 275 kV / 132 kV to investigate the tripping pattern and arrester placement.

REFERENCES

- CIGRE WG 33-01. (October, 1991). Guide To Procedures For Estimating The Lightning Performance Of Transmission Lines: CIGRE.
- Ametani, A., & Kawamura, T. (2005). A Method of a Lightning Surge Analysis Recommended In Japan Using EMTP. *IEEE Transactions on Power Delivery*, 20(2), 867-875.
- Applications of PSCAD/EMTDC. (2007). Manitoba Canada: Manitoba HVDC Research Centre Inc.
- Armstrong, HR, & Whitehead, Edwin R. (1968). Field and analytical studies of transmission line shielding. *IEEE Transactions on Power Apparatus and Systems* (1), 270-281.
- Azizan, H. (2010). On lightning watch. <http://www.thestar.com.my/Story/?file=%2F2010%2F3%2F7%2Ffocus%2F5808493&sec=focus>. Accessed on January 2014.
- Bakar, A. H. A. , Talib, D. N. A., Mokhlis, H., & Illias, H. A. (2013). Lightning Back Flashover Double Circuit Tripping Pattern of 132 kV Lines in Malaysia. *International Journal of Electrical Power & Energy Systems*, 45(1), 235-241.
- Bakar, A.H.A., Othman, M.R. , & Osman, H. (2007). Economic Positioning of Line Lightning Arresters Based on Observation and Analysis of Lightning Surges. *Cigre Symposium on Transient Phenomena in Large Electric Power System*, Zagreb Croatia.
- Bergeron, L. (2009). *Water Hammer in Hydraulics and Waze Surges in Electricity*, 1961: John Wiley, New York) [translated from the original French text, 1950 (Dunod, Paris)].
- Brown, Gordon W, & Whitehead, Edwin R. (1969). Field and analytical studies of transmission line shielding. *IEEE Transactions on Power Apparatus and Systems* (5), 617-626.
- Bruce, C.E.R., & Golde, R.H. (1941). The Lightning Discharge. *Journal of Institution of Electrical Engineering*, 88, 487-520.
- Chowdhuri, Pritindra. (2001). Parameters of lightning strokes and their effects on power systems. *IEEE/PES Transmission and Distribution Conference and Exposition*.
- Christodoulou, CA, Ekonomou, L, Mitropoulou, AD, Vita, V, & Stathopoulos, IA. (2010). Surge arresters' circuit models review and their application to a Hellenic 150kV transmission line. *Simulation Modelling Practice and Theory*, 18(6), 836-849.

- Darveniza, M. (1988). The generalized integration method for predicting impulse volt-time characteristics for non-standard wave shapes-A theoretical basis. *IEEE Transactions on Electrical Insulation*, 23(3), 373-381.
- Dezelak, K, Stumberger, G, & Jakl, Franc. (2010). Arrangements of overhead power line conductors related to the electromagnetic field limits. *Proceedings of the International Symposium Modern Electric Power Systems (MEPS)*.
- Dommel, H.W. (1986). *Electromagnetic Transients Program (EMTP) Theory Book: Bonneville Power Administration*.
- Gazzana, D. S., Bretas, A. S., Dias, G. A., Tello, M., Thomas, D. W., & Christopoulos, C. (2014). The Transmission Line Modeling Method to Represent the Soil Ionization Phenomenon in Grounding Systems. *IEEE Transactions on Magnetics*, 50(2), 505-508.
- Gouda, O. E., El Dein, A. Z., & Amer, G. M. (2010). Parameters Affecting the Back Flashover Across the Overhead Transmission Line Insulator Caused by Lightning. *MEPCON'10*, Cairo.
- Group, IEEE Working. (1985). A simplified method for estimating lightning performance of transmission lines. *IEEE Transactions on Power Apparatus System*, 104(4), 919-932.
- Hayashi, Tomohiro, Mizuno, Yukio, & Naito, Katsuhiko. (2008). Study on Transmission Line Arresters for Tower with High Footing Resistance. *IEEE Transactions on Power Delivery*, 23(4), 2456-2460.
- Heidler, F, & Cvetić, J. (2002). A class of analytical functions to study the lightning effects associated with the current front. *European Transactions on Electrical Power*, 12(2), 141-150.
- Hileman, A. R. (1999). *Insulation Coordination for Power System: Taylor & Francis Group*.
- IEC, TR. (2004). 60071-4, *Insulation Co-ordination Part 4*.
- IEEE Guide for the Application of Insulation Coordination. (1999). *IEEE Std 1313.2-1999*.
- IEEE Std 1243-1997. (1997). *IEEE Guide for Improving the Lightning Performance of Transmission Lines*. doi: 10.1109/IEEESTD.1997.84660
- IEEE Std C62.22. (2009). *IEEE Guide for the Application of Metal-Oxide Surge Arresters for Alternating-Current Systems*. *IEEE Std C62.22-2009*, 1-131.
- IEEE Working Group 3.4.11. (1992). Modeling of Metal Oxide Surge Arresters. *IEEE Transactions on Power Delivery*, 7(1), 302-309.

- Ishii, M., & Kawamura, H. (2011, 3-7 Oct. 2011). Application of line surge arresters to double-circuit transmission lines. International Symposium on Lightning Protection.
- Ito, T., Ueda, T., Watanabe, H., Funabashi, T., & Ametani, A. (2003). Lightning Flashovers on 77 kV Systems: Observed Voltage Bias Effects and Analysis. IEEE Transactions on Power Delivery, 18(2), 545-550.
- Love, ER. (1973). Improvements in lightning stroke modeling and applications to design of EHV and UHV transmission lines. MSc, University of Colorado, Denver, CO.
- Malcolm, N., & Aggarwal, R. (2014). An analysis of reducing back flashover faults with surge arresters on 69/138 kV double circuit transmission lines due to direct lightning strikes on the shield wires. IET International Conference on Developments in Power System Protection.
- Marti, José R. (1982). Accurate modelling of frequency-dependent transmission lines in electromagnetic transient simulations. IEEE Transactions on Power Apparatus and Systems (1), 147-157.
- Martinez-Velasco, Juan A. (2010). Power Systems Transients: Parameter Determination. Boca Raton: CRC Press.
- Martinez, JA, Gustavsen, B, & Durbak, D. (2005). Parameter determination for modeling system transients-Part I: Overhead lines. IEEE Transactions on Power Delivery, 20(3), 2038-2044.
- McDermott, T. E. (2006). Line Arrester Energy Discharge Duties. Proceedings of IEEE Power Engineering Society on Transmission and Distribution, Dallas.
- Munukutla, K., Vittal, V., Heydt, G. T., Chipman, D., & Keel, B. (2010). A Practical Evaluation of Surge Arrester Placement for Transmission Line Lightning Protection. IEEE Transactions on Power Delivery, 25(3), 1742-1748.
- Nourai, A., Keri, A. J. F., & Shih, C. H. (1988). Shield wire loss reduction for double circuit transmission lines. IEEE Transactions on Power Delivery, 3(4), 1854-1864.
- Nucci, C.A. (2009). A Survey on Cigré And IEEE Procedures For The Estimation Of The Lightning Performance Of Overhead Transmission And Distribution Lines. International Symposium on Lightning Protection, Curitiba, Brazil.
- Pham, T.H., Boggs, S.A., Suzuki, H., & Imai, T. (2012). Effect of Externally Gapped Line Arrester Placement on Insulation Coordination of a Twin-Circuit 220 kV Line. IEEE Transactions on Power Delivery, 27(4), 1991-1997.

- Pinto, A. J. G., Costa, E. C. M., Kurokawa, S., Monteiro, J. H. A., de Franco, J. L., & Pissolato, J. (2014). Analysis of the electrical characteristics and surge protection of EHV transmission lines supported by tall towers. *International Journal of Electrical Power & Energy Systems*, 57(0), 358-365.
- Rawi, I., & Ab Kadir, M. (2014). Procedures for evaluating the HV overhead lines lightning performance and methods for reducing the OHL trip rate in TNB transmission. *IEEE International Power Engineering and Optimization Conference (PEOCO)*.
- Sadovic, T., & Sadovic, S. (2009). EMTP_RV Modelling for the Transmission Line Lightning Performance Computation. User Group Meeting.
- Saengsirwan, T., & Thipprasert, W. (2004, 21-24 Nov. 2004). Lightning arrester modeling using ATP-EMTP. *IEEE Region 10 Conference TENCON*.
- Sardi, J., & Chian, J. O. C. (2010). Evaluation of surge arrester requirement for overhead transmission line using Electromagnetic Transient Program. *IEEE International Conference on Power and Energy (PECON)*.
- Sardi, J., Kadir, M. Z. A.A., Ahmad, W., Hizam, H., Rawi, I., Mohamed, Ahmad, A. (2008). Backflashover analysis for 132 kV Kuala Krai-Gua Musang transmission line. *IEEE International Power and Energy Conference, PECON*.
- Savic, Milan S. (2005). Estimation of The Surge Arrester Outage Rate Caused By Lightning Overvoltages. *IEEE Transactions on Power Delivery*, 20(1), 116-122.
- Talib, D. N. A., Bakar, Ah A., & Mokhlis, H. (2012, 2-5 Dec. 2012). Parameters affecting lightning backflash over pattern at 132kV double circuit transmission lines. *IEEE International Conference on Power and Energy (PECON)*.
- Taniguchi, S., Tsuboi, T., Okabe, S., Nagaraki, Y., Takami, J., & Ota, H. (2010). Method of Calculating the Lightning Outage Rate Of Large-Sized Transmission Lines. *IEEE Transactions on Dielectrics and Electrical Insulation* 17(4), 1276-1283.
- Tarasiewicz, Eva J, Rimmer, Finn, & Morched, Atef S. (2000). Transmission Line Arrester Energy, Cost, And Risk Of Failure Analysis For Partially Shielded Transmission Lines. *IEEE Transactions on Power Delivery*, 15(3), 919-924.
- Uman, M.A. (2001). *The Lightning Discharge: Dover Publications*.
- Wagner, CF, & Hileman, AR. (1961). The lightning stroke-II. Power Apparatus and Systems, Part III. *Transactions of the American Institute of Electrical Engineers* 80(3), 622-636.
- Whitehead, James T, Chisholm, William A, Anderson, JG, Clayton, R, Elahi, H, Eriksson, A.J., Longo, V.J. (1993). *IEEE working group report. Estimating*

lightning performance of transmission lines. II: Updates to analytical models. IEEE transactions on Power Delivery, 8(3), 1254-1267.

Woodworth, J. (Producer). (2008). Understanding The Energy Handling Issue. http://www.arresterworks.com/arresterfacts/pdf_files/understanding_arrester_energy_handling.pdf, Accessed in February 2014.

Woodworth, J. (Producer). (2009). What is a Transmission Line arrester. Retrieved from http://www.arresterworks.com/ArresterFacts_files/ArresterFacts%20017%20What%20is%20a%20Transmission%20Line%20Arrester.pdf

World Lightning Map. (2014). http://www.lightningsafety.com/nlsi_info/lightning_maps/worldlightning.html, Accessed in August 2013.

Xi, W., Li, Z., & He, J. (2014). Improving the lightning protection effect of multi-circuit tower by installing coupling ground wire. Electric Power Systems Research, 113, 213-219.

You, M., Zhang, B.H., Cheng, L.Y., Bo, Z.Q., & Klimek, A. (2010). Lightning Model for HVDC Transmission Lines. IET International Conference on Developments in Power System Protection, Manchester, UK.

University of Malaya

APPENDIX B

List of ISI journal publications:

1. N. H. N. Hassan, S. A. Halim, A. H. A. Bakar, H. A. Illias, H. Mokhlis, "Analysis of discharge energy on surge arrester configurations in 132 kV double circuit transmission lines," Journal of Measurement (under review).

List of conference paper publications:

1. Nor Hidayah Nor Hassan, Ab. Halim Abu Bakar, Hazlie Mokhlis, Hazlee Azil Illias, "Analysis of Arrester Energy for 132kV Overhead Transmission Line due to Back Flashover & Shielding Failure ," 2012 IEEE International Conference on Power and Energy (PECON 2012), 2nd to 5th December 2012, Kota Kinabalu, Sabah, Malaysia.